JOURNAL OF PETROLOGY | VOLUME 49 | NUMBER 4 | PAGES 665–695 | 2008 | doi:10.1093/petrology/egm069

Insights into Petrological Characteristics of the Lithosphere of Mantle Wedge beneath Arcs through Peridotite Xenoliths: a Review

SHOJI ARAI* AND SATOKO ISHIMARU

DEPARTMENT OF EARTH SCIENCES, KANAZAWA UNIVERSITY, KANAZAWA 920-1192, JAPAN

RECEIVED DECEMBER 8, 2006; ACCEPTED OCTOBER 12, 2007
ADVANCE ACCESS PUBLICATION NOVEMBER 22, 2007

The petrological characteristics of peridotite xenoliths exhumed from the lithospheric mantle below the Western Pacific arcs (Kamchatka, NE Japan, SW Japan, Luzon–Taiwan, New Ireland and Vanuatu) are reviewed to obtain an overview of the supra-subduction zone mantle in mature subduction systems. These data are then compared with those for peridotite xenoliths from recent or older arcs described in the literature (e.g. New Britain, Western Canada to USA, Central Mexico, Patagonia, Lesser Antilles and Pannonian Basin) to establish a petrological model of the lithospheric mantle beneath the arc. In currently active volcanic arcs, the degree of partial melting recorded in the peridotites appears to decrease away from the fore-arc towards the back-arc region. Highly depleted harzburgites, more depleted than abyssal harzburgites, occur only in the frontal arc to fore-arc region. The degree of depletion increases again to a degree similar to that of the most depleted abyssal harzburgites within the back-arc extensional region, whether or not a back-arc basin is developed. Metasomatism is most prominent beneath the volcanic front, where the magma production rate is highest; silica enrichment, involving the metasomatic formation of secondary orthopyroxene at the expense of olivine, is important in this region because of the addition of slab-derived siliceous fluids. Some apparently primary orthopyroxenes, such as those in harzburgites from the Lesser Antilles arc, could possibly be of this secondary paragenesis but have been recrystallized such that the replacement texture is lost. The Ti content of hydrous minerals is relatively low in the sub-arc lithospheric mantle peridotites. The K/Na ratio of the metasomatic hydrous minerals decreases rearward from the fore-arc mantle as well as downward within the lithospheric mantle. The lithospheric mantle wedge peridotites, especially metasomatized ones from below the volcanic front, are highly oxidized. Shearing of the mantle wedge is expected beneath the volcanic front, and is represented by fine-grained peridotite xenoliths.

KEY WORDS: *mantle wedge; lithospheric mantle; peridotite xenoliths; melting; metasomatism*

INTRODUCTION

The mantle wedge above a subducting slab is an important locus for magma generation, ultimately contributing to the growth of the continental crust. It is expected to have a complex mineralogy and bulk-rock composition as a consequence of material input from the subducted slab combined with continual magmatic discharge upward. Mantle-wedge materials are relatively under-sampled as peridotite xenoliths (e.g. Nixon, 1987), and have been less thoroughly investigated than mantle xenoliths from the other tectonic settings, such as continental rift zones and oceanic hotspots. It is well known that subduction-related magmas have distinct geochemical characteristics compared with those of other tectonic settings (e.g. Pearce & Cann, 1973). Mantle peridotites can also be discriminated in terms of tectonic setting to some extent. For example, some mantle-wedge peridotites appear to have experienced higher degrees of partial melting than abyssal peridotites (e.g. Dick & Bullen, 1984; Arai, 1994), and exhibit higher oxygen fugacities on average than abyssal peridotites (e.g. Ballhaus *et al.*, 1991; Parkinson & Arculus, 1999).

*Corresponding author. Telephone: 81-76-264-6521. Fax: 81-76-264-6545. E-mail: ultrasa@kenroku.kanazawa-u.ac.jp

Mantle-wedge peridotites, however, appear to have complex petrographical characteristics (e.g. Arai *et al.*, 2004; Ishimaru *et al.*, 2007), and an updated summary is needed for our better understanding of their petrogenesis.

The Western Pacific region is ideal for understanding mantle-wedge petrology, because it has a number of subduction systems with a significant number of xenolith localities that occur at variable depths above the subducting slab. There is clear across-arc polarity in terms of magma chemistry (e.g. Kuno, 1966), amount of magma supply (e.g. Sugimura *et al.*, 1963) and material input from the slab (e.g. Tatsumi, 1986), which depends on the depth to the subducted slab. We can, therefore, examine the petrological characteristics of the mantle beneath the arc in response to this polarity. We first summarize the characteristics of peridotite xenoliths from the Western Pacific using data from the literature and our own unpublished data, and then compare their petrological characteristics with peridotite xenoliths from other localities of possible mantle-wedge origin. We mainly focus on the major-element chemistry of the common peridotite minerals (olivine, ortho- and clinopyroxenes, chromian spinel and hydrous minerals); the trace-element mineral chemistry and glass chemistry will be discussed elsewhere. Arai *et al.* (1998, 2000, 2007) and Abe *et al.* (1999) have provided detailed descriptions of the peridotite xenoliths from the Japan arcs and the Western Pacific region, respectively. The host volcanic rocks to the xenoliths are mainly of Cenozoic age so that we can reconstruct the tectonic setting of the mantle from which they were derived.

Peridotite xenoliths from a locality are basically derived from the lithospheric mantle; this may have been formed from asthenospheric mantle by cooling in the present tectonic setting, or may have been modified from pre-existing lithospheric mantle formed in a previous setting through metasomatism by agents from the underlying asthenosphere or subducted slab, if any. They can provide us with information on melting and metasomatic processes within the upper mantle. We refer to the 'lithospheric mantle peridotite' beneath arcs, including the fore-arc and back-arc regions, as the 'mantle-wedge peridotite' in this paper.

PETROLOGICAL SUMMARY OF PERIDOTITE XENOLITHS FROM THE WESTERN PACIFIC ARCS

There are many xenolith localities of likely mantle-wedge origin in the Western Pacific region (e.g. Arai *et al.*, 2007) (Fig. 1). They are grouped into five regions for the purpose of this study; these are, from north to south, the Kamchatka arc, NE Japan arc, SW Japan arc, Luzon–Taiwan arc and southwestern Pacific arcs (Papua New Guinea to Vanuatu). It is noteworthy that the xenoliths, except those from the SW Japan arc, are entrained in magmas of arc affinity, which were generated within the supra-subduction zone mantle wedge (see Arai *et al.*, 1996). On the other hand, the xenoliths from the SW Japan arc hosted in alkali basalts of intraplate affinity, whose petrogenesis has been related to the formation of a slab window during the waning stage of Japan Sea (back-arc basin) opening (e.g. Uto, 1990; Iwamori, 1991). Subduction-related components were involved in the petrogenesis of the host alkali basalt magmas to variable extents (Nakamura *et al.*, 1990). The peridotite xenoliths from the SW Japan arc represent fragments of lithospheric mantle modified to various degrees by infiltration of intraplate magmas (e.g. Arai *et al.*, 2000, 2007). In addition, we report data for mantle xenolith localities within the Sea of Japan, one of the back-arc basins of the Western Pacific, including Oki-Dogo island, which has been interpreted as a remnant of continental lithosphere off the coast of Honshu (Takahashi, 1978*a*; Abe *et al.*, 2003). Ninomiya *et al.* (2007) reported peridotite xenoliths from a small seamount in the Sea of Japan.

Peridotite xenoliths from the Avacha (Avachinsky) volcano in the southern part (e.g. Swanson *et al.*, 1987; Kepezhinskas & Defant, 2001; Arai *et al.*, 2003; Ishimaru *et al.*, 2007) and from the Valovayam Volcanic Field (VVF) in the northern part (Kepezhinskas *et al.*, 1995) are the most famous and best studied of all peridotite xenolith suites from the Kamchatka arc, Russia. Bryant *et al.* (2007) described ultramafic xenoliths from Shiveluch volcano in the central Kamchatka arc (Fig. 1). Only two localities, Megata and Oshima-Ôshima volcanoes, are known in which peridotite xenoliths are exhumed within the NE Japan arc. Ultramafic xenoliths from the Ichinomegata crater of the Megata volcano have been extensively studied (e.g. Aoki, 1987; Takahashi, 1980, 1986). In contrast, there are many mantle xenolith localities in the SW Japan arc (e.g. Takamura, 1973; Takahashi, 1978*a*; Arai *et al.*, 2000). Takashima and Kurose in northern Kyushu (e.g. Arai *et al.*, 2000, 2007) and Noyamadake in western Honshu (e.g. Abe *et al.*, 1999; Arai *et al.*, 2000), among them, provide abundant mantle xenoliths, which record a variety of mantle-wedge processes. The Iraya volcano, Batan Island, of the Luzon–Taiwan arc, is famous for its abundant mantle peridotite xenoliths (Richard, 1986; Vidal *et al.*, 1989; Maury *et al.*, 1992; Arai *et al.*, 2004). The TUBAF seamount near Lihir Island of the New Ireland arc, Papua New Guinea (Fig. 1), is famous for metasomatized peridotite xenoliths (Franz & Wirth, 2000; McInnes *et al.*, 2001; Franz *et al.*, 2002). The xenoliths are hosted in Quaternary trachybasalts generated by rifting of the fore-arc region of the Tertiary New Ireland (or Tabar–Lihir–Tanga–Feni) arc

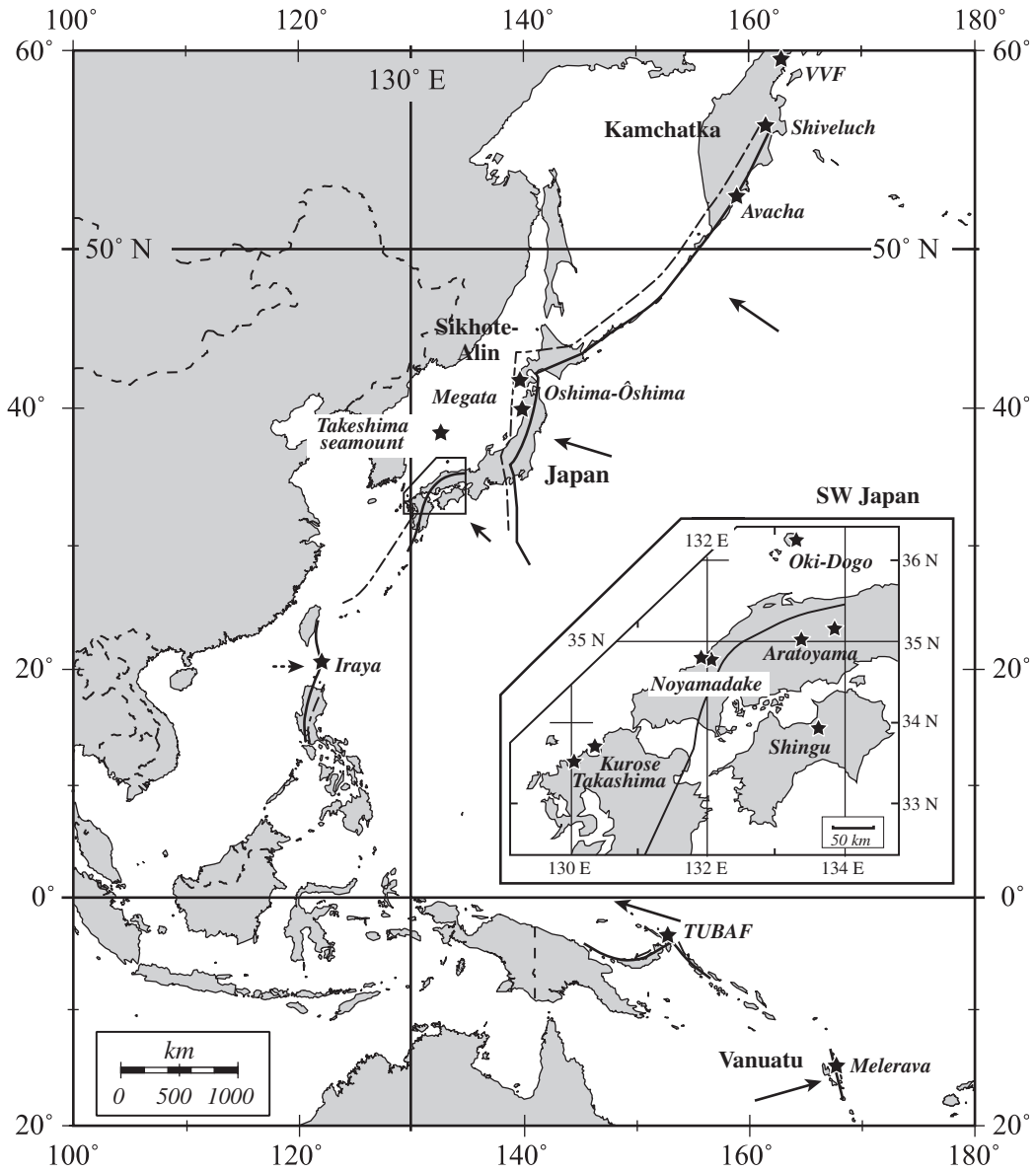

Fig. 1. Location map of the main peridotite xenolith localities (black stars) in the Western Pacific. Volcanic front (bold continuous line) and 200 km depth contour of the subducting slab (dash–dot line) are constructed from the data of Yoshii (1979), Cardwell *et al.* (1980) Barsdell & Smith (1989), Cooper & Taylor (1989), Lewis & Hayes (1989), Tatsumi *et al.* (1994), Gorbatov *et al.* (1997), Wallace *et al.* (2004), van Ufoord & Cloos (2005) and Kimura & Yoshida (2006). Volcanic fronts are shown only where the plate boundaries are complicated. Subducting plate motions are shown approximately by arrows (Minster *et al.*, 1974; DeMets *et al.*, 1990; Turner *et al.*, 1999; Wallace *et al.*, 2004). Data sources: Kepezhinskas *et al.* (1995) for VVF (Valovayam Volcanic Field), Bryant *et al.* (2007) for Shiveluch, Ishimaru *et al.* (2007) for Avacha, Ninomiya & Arai (1992) for Oshima-Ôshima, Takahashi (1980) for Megata, Ninomiya *et al.* (2007) for Takeshima seamount, Takahashi (1978*a*, 1978*b*) for Oki-Dogo, Arai *et al.* (2000) for Aratoyama, Takashima and Kurose, Goto & Arai (1987) for Shingu, Arai *et al.* (2004) for Iraya, Franz *et al.* (2002) for TUBAF, and Barsdell & Smith (1989) for Merelava (Vanuatu).

(McInnes & Cameron, 1994; Franz *et al.*, 2002). Barsdell & Smith (1989) found wehrlite and harzburgite xenoliths in primitive olivine tholeiite lavas of arc affinity erupted from Merelava volcano, in the Vanuatu (New Hebrides) arc (Fig. 1). Merelava volcano is located slightly rearward from the volcanic front formed by the main Vanuatu volcanic chain (Barsdell & Smith, 1989).

Peridotite xenoliths, enclosed by 8 Ma alkali basalt from the Takeshima seamount (Fig. 1; Ninomiya *et al.*, 2007) are considered representative of the upper mantle beneath the Sea of Japan, which opened rapidly at around 15 Ma (e.g. Otofuji *et al.*, 1985) and is one of the back-arc basins characteristic of the Western Pacific (Tamaki & Honza, 1991). The xenoliths are very small, <3 cm across,

and range in composition from harzburgite to lherzolite (Ninomiya *et al.*, 2007).

The current margin of the Eurasian continent (e.g. Sikhote-Alin, Far East Russia; Fig. 1), has been a long-lived convergent continental margin (e.g. Faure & Natal'n, 1992); some of the ultramafic xenoliths are derived from continental lithosphere affected by supra-subduction zone metasomatism (e.g. Ionov *et al.*, 1995; Yamamoto *et al.*, 2004). These xenoliths are excluded from this study because they mainly exhibit subcontinental lithospheric mantle signatures in terms of their mineral chemistry (e.g. Arai *et al.*, 2007). No harzburgite to lherzolite xenoliths have been reported from the Aleutian arc, although dunite, wehrlite and clinopyroxenite xenoliths are found in calc-alkaline andesites from Adak island (Conrad & Kay, 1984; Debari *et al.*, 1987), and dunite xenoliths are found in alkaline basalts from Kanaga island (DeLong *et al.*, 1975). All of these Aleutian xenoliths are closely associated with mafic xenoliths and are interpreted to be of cumulus origin; they do not, therefore, provide direct information about the upper mantle.

Petrography

No garnet-bearing peridotite xenolith has been found in any of the arcs in the Western Pacific listed above (see Abe & Arai, 2001). Plagioclase-bearing spinel lherzolite occurs only within the Megata xenolith suite (Ichinomegata crater) in the NE Japan arc (e.g. Takahashi, 1986). Almost all the peridotite xenoliths are spinel-bearing varieties without garnet or plagioclase. The range of petrographic characteristics of the peridotite xenoliths from the Western Pacific arcs is illustrated in Fig. 2.

The peridotite xenoliths from the Avacha and Iraya volcanoes are harzburgites with very low contents of clinopyroxene (Fig. 3a and d). The Avacha harzburgites are especially poor in clinopyroxene (Figs 2a and 3a). Dunites and pyroxenites are relatively infrequent as xenoliths in these localities. The peridotite xenoliths from the NE and SW Japan arcs range from depleted harzburgite to lherzolite (Fig. 3b and c). Xenoliths of dunite and pyroxenite of the green-pyroxene series [equivalent to the Group I xenoliths of Frey & Prinz (1978)] are commonly associated (Fig. 3b and c). Websterites are dominant, but clinopyroxenites and orthopyroxenites are also commonly found (Fig. 3b and c; Arai *et al.*, 2000). In the SW Japan arc, a large number of black-pyroxene series xenoliths [Group II xenoliths of Frey & Prinz (1978)] are found as discrete xenoliths or megacrysts, or as composite xenoliths with peridotites and pyroxenites of Group I (e.g. Arai *et al.*, 2000, 2007).

The TUBAF peridotite xenoliths from the New Ireland arc, Papua New Guinea (Fig. 1), are characterized by relatively high amounts of olivine (Fig. 3e). Some pyroxenes, especially orthopyroxenes forming radial aggregates, appear to have been formed at the expense of olivine. Some of the peridotites contain high amounts of clinopyroxene relative to orthopyroxene (Fig. 3e) as a consequence of metasomatic modification (Franz *et al.*, 2002), suggesting that the initial peridotite was a depleted harzburgite to dunite.

The harzburgites from Merelava volcano, although interpreted as fragments of ophiolitic mantle (Barsdell & Smith, 1989), exhibit no sign of low-temperature alteration (serpentinization) and are similar to the metasomatized harzburgite xenoliths from Avacha and Iraya (Barsdell & Smith, 1989, fig. 3; Arai *et al.*, 2004; Ishimaru *et al.*, 2007). We propose here that the Merelava harzburgites are representative of the lithospheric mantle beneath an oceanic arc, the Vanuatu arc.

Some of the peridotite xenoliths from the Megata volcano (Ichinomegata crater) are famous for containing secondary metasomatic hydrous minerals; that is, pargasite and phlogopite (e.g. Aoki & Shiba, 1973; Arai, 1986) (Fig. 2f). The hydrous minerals are colorless to light brown in thin section, replacing mainly clinopyroxenes that form exsolution lamellae in orthopyroxene porphyroclasts and spinel–pyroxene symplectites (e.g. Arai, 1986) that are subsolidus products (Takahashi, 1986). Fine-grained peridotites from the Iraya and Avacha volcanoes commonly contain amphiboles (Fig. 2e), which are variable in composition from pargasite to tremolite, closely associated with secondary orthopyroxene as described below (Ishimaru *et al.*, 2007; Ishimaru & Arai, 2008).

The peridotites from Avacha, Shiveluch and Iraya characteristically contain secondary orthopyroxene replacing olivine (Arai & Kida, 2000; Arai *et al.*, 2003, 2004; Bryant *et al.*, 2007; Ishimaru *et al.*, 2007) (Fig. 2b and d). The secondary orthopyroxene shows no deformation or exsolution textures, and sometimes forms radial aggregates (e.g. Arai & Kida, 2000; Arai *et al.*, 2004). The secondary orthopyroxene is only rarely associated with other silicates of metasomatic origin (Fig. 2b and d); stout secondary orthopyroxene usually accompanies pargasite and glass in the Avacha peridotites (Ishimaru *et al.*, 2007). This type of metasomatism (i.e. formation of the secondary orthopyroxene at the expense of olivine) enhances the total orthopyroxene content of the peridotite (Arai *et al.*, 2004; Bryant *et al.*, 2007; Ishimaru *et al.*, 2007), and thus enriches the peridotite in silica (e.g. Fig. 3a).

Some peridotite xenoliths, especially the metasomatized ones, from the Western Pacific arcs contain sulfides (e.g. Hattori *et al.*, 2002; Arai *et al.*, 2003) (Fig. 2f). The sulfides are closely associated with metasomatic minerals such as secondary pargasite in the peridotite xenoliths from the Ichinomegata crater of the Megata volcano, the NE Japan arc (Hattori *et al.*, 2002) (Fig. 2f). Some peridotite xenoliths, especially metasomatized peridotite xenoliths from Avacha, Kamchatka arc (Arai *et al.*, 2003; Ishimaru *et al.*, 2007), contain monomineralic sulfide globules.

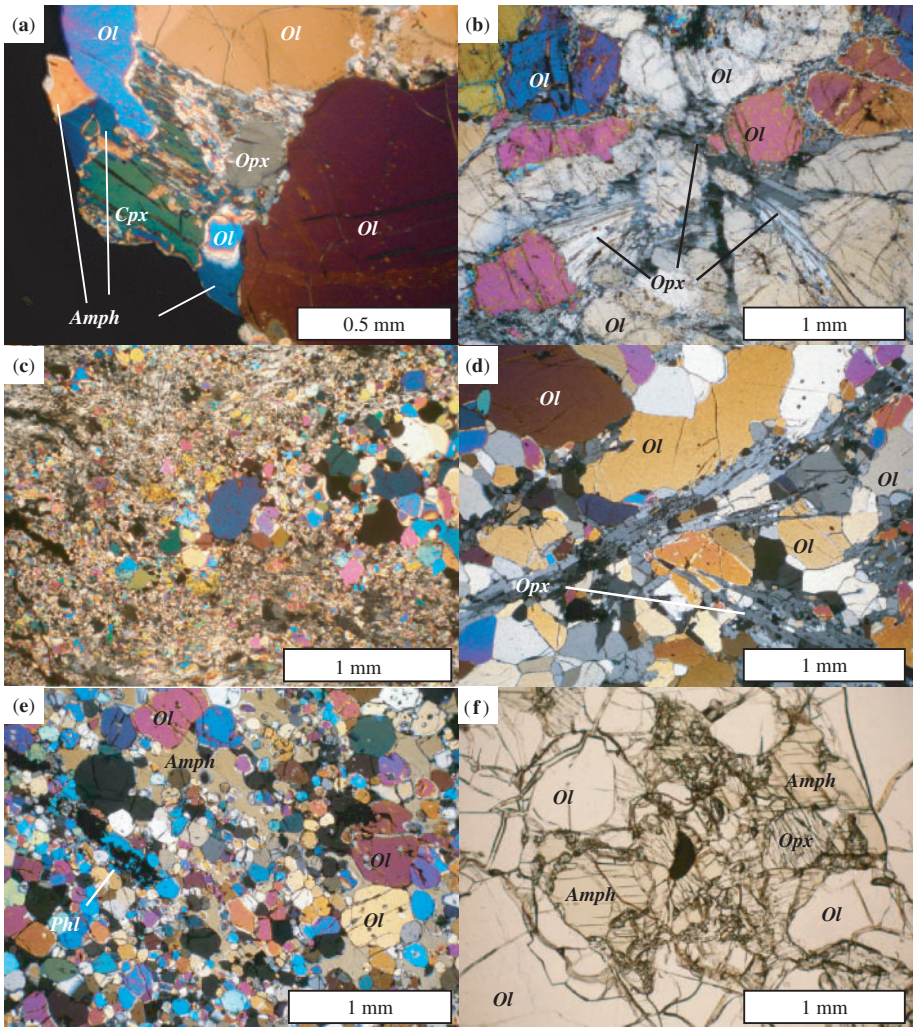

Fig. 2. Photomicrographs of peridotite xenoliths with characteristic textures from some Western Pacific arcs; Avacha volcano, Kamchatka arc (a–c); Iraya volcano (Batan Island), Luzon–Taiwan arc, Philippines (d, e) and Megata volcano, NE Japan arc (f). CP, crossed-polarized transmitted light; PP, plane-polarized transmitted light. Ol, olivine; Opx, orthopyroxene; Cpx, clinopyroxene; Amph, amphibole; Phl, phlogopite. (a) Discrete amphibole (pargasite), which is possibly primary, in a coarse-grained peridotite xenolith (sample 200). CP. (b) Secondary orthopyroxene replacing olivine in a coarse-grained part of a composite xenolith (sample 166), composed of fine-grained and coarse-grained peridotite. It should be noted that the secondary orthopyroxene forms fibrous radial aggregates. CP. (c) Fine-grained peridotite (fine-grained part of sample 166). The extremely fine grains of olivine should be noted. CP. (d) Secondary orthopyroxene replacing olivine in a fine-grained part of peridotite (sample 64-9-3). The orthopyroxene also forms fibrous radial aggregates (see b). CP. (e) Fine-grained peridotite (sample 60–12). Fine chromian spinel aggregates are frequently surrounded by phlogopite and/or amphibole. CP. (f) Relatively coarse-grained peridotite (sample Ich-006). The sulfide grain (central, black) surrounded by amphibole should be noted. PP.

The presence of fine-grained peridotite xenoliths is one of the characteristics of the Western Pacific arcs (Arai *et al.*, 2007) (Fig. 2c and e). Intense metasomatism was involved in the formation of the fine-grained peridotites (Ishimaru *et al.*, 2007; Ishimaru & Arai, 2008), which do not belong any type of peridotite previously described (Mercier & Nicolas, 1975; Harte, 1977). The fine-grained peridotite xenoliths from the Shiveluch volcano (Bryant *et al.*, 2007, fig. 3) are very similar to those from Avacha (Fig. 2c). The peridotite xenolith suite from the Iraya volcano of the Luzon–Taiwan arc is dominated by fine-grained types (Arai *et al.*, 1996) (Fig. 2e). Rare composite xenoliths of coarse-grained and fine-grained peridotite are found at the Avacha volcano, Kamchatka arc (Ishimaru *et al.*, 2007; Ishimaru & Arai, 2008).

Mineral chemistry

The mineral chemical characteristics of the xenoliths are summarized here. Mg-number is the $Mg/(Mg+Fe^{2+})$ atomic ratio, and Cr-number is the $Cr/(Cr+Al)$ atomic ratio. γ_{Cr}, γ_{Al} and γ_{Fe} are the atomic fractions of Cr, Al and Fe^{3+}, respectively, relative to total trivalent cations

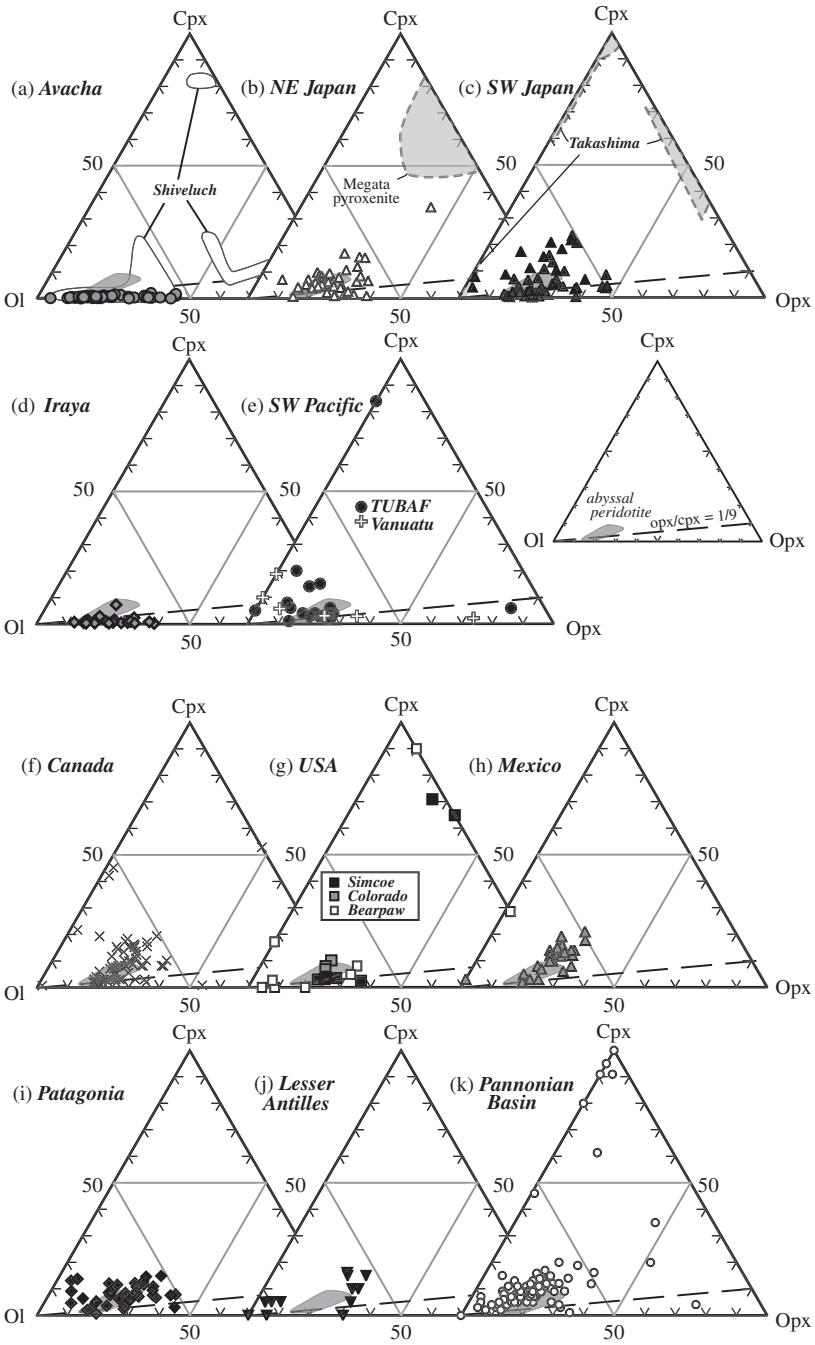

Fig. 3. Modal compositions of ultramafic xenoliths from the mantle wedge. The field of abyssal peridotites (Dick *et al.*, 1984) is shown for reference. Dashed line denotes Cpx/(Opx + Cpx) = 0·1; this may be a genetic boundary between lherzolite and harzburgite, which are Cpx-bearing and Cpx-free, respectively, at solidus temperatures (see Arai, 1984). (a) Avacha volcano, the Kamchatka arc. Data from Ishimaru (2004). Ultramafic xenoliths from Shiveluch, central Kamchatka (Bryant *et al.*, 2007) are shown for comparison. (b) NE Japan arc (Megata volcano). Data from Abe (1997) and Abe *et al.* (1992). The field of pyroxenite xenoliths is shown (Arai, 1980). (c) SW Japan arc. Data from Hirai (1986), Abe (1997) and Abe *et al.* (2003). The field of pyroxenite and dunite xenoliths from Takashima (Arai *et al.*, 2001) is shown for comparison. (d) Iraya volcano, Batan Island, the Luzon–Taiwan arc. Data from Kida (1998). (e) Southwestern Pacific. Data for TUBAF seamount, the New Ireland arc, Papua New Guinea are from McInnes *et al.* (2001) and Franz *et al.* (2002). Data for Merelava volcano, Vanuatu, are from Barsdell & Smith (1989). (f) Canadian Cordillera. Data from Francis (1987), Peslier *et al.* (2002) and Harder & Russell (2006). (g) Western USA. Data from Brandon & Draper (1996) for Cascades, from Smith & Riter (1997) and Smith *et al.* (1999) for the Colorado Plateau, and from Downes *et al.* (2004) for Bearpaw. (h) Central Mexico. Data from Luhr & Aranda-Gómez (1997) and Blatter & Carmichael (1998). (i) Patagonia. Data from Rivalenti *et al.* (2004*a*, 2004*b*) and Schilling *et al.* (2005). (j) Lesser Antilles. Data from Parkinson *et al.* (2003). (k) Pannonian Basin, central Europe. Data from Szabó & Taylor (1994), Downes *et al.* (1995), Szabó *et al.* (1995), Vaselli *et al.* (1995) and Bali *et al.* (2002).

($Cr + Al + Fe^{3+}$), in chromian spinel. All iron is assumed to be Fe^{2+} in silicates. Fe^{2+} and Fe^{3+} in chromian spinel were calculated assuming spinel stoichiometry. Fo content in olivine is 100Mg-number.

The peridotite xenoliths from the Avacha volcano have depleted mineral chemistries (Figs 4a, 5a and 6a) in accordance with their clinopyroxene-poor mode (Fig. 2a). Most of the primary chromian spinels exhibit high Cr-number, >0·5, indicating a degree of melting higher than that in abyssal peridotites (Figs 4a, 5a and 6a). The Iraya harzburgite is also more depleted, on average, in terms of its mineral chemistry compared with abyssal peridotites (Fig. 4d), consistent with the low clinopyroxene content (Fig. 3d). In contrast, the peridotite xenoliths from the NE and SW Japan arcs have similar Fo contents (olivine) and Cr-number values (chromian spinel) to abyssal peridotites, except for some harzburgite xenoliths from Noyamdake, which are as depleted as those from Avacha and Iraya (Fig. 4a–c). Some peridotite xenoliths that are closely associated with Group II (black-pyroxene series) pyroxenites and megacrysts from Shingu and Aratoyama (SW Japan arc) have lower Fo contents of olivine than those free from the association (Kurose and Noyamadake) at a given Cr-number of spinel (Fig. 4c; Arai *et al.*, 2000). The unmetasomatized TUBAF peridotites (e.g. the peridotites plotting within the olivine–spinel mantle array; Fig. 4e), contain high-Cr-number (>0·5) chromian spinel (Figs 4e, 5e and 6e). Some of the TUBAF metasomatized peridotite xenoliths plot off the olivine–spinel mantle array and contain olivines less magnesian than typical mantle olivines at a given Cr-number of spinel (Fig. 4e). Others contain magnesian olivines and low-Cr-number (almost zero) spinels (Fig. 4e). Olivines in the Vanuatu peridotite xenoliths are slightly less magnesian than residual mantle olivine at a high (>0·7) Cr-number of spinel (Fig. 4e).

Chromian spinels in the mantle-wedge peridotite xenoliths from the Western Pacific generally show an Fo (olivine)–Cr-number (spinel) trend similar to the abyssal peridotite trend, although some harzburgites from Kamchatke, Iraya, Noyamadake, TUBAF and Merelava (Vanuatu) contain high-Cr-number spinels that plot outside the abyssal peridotite field (Fig. 4a, b and d). The metasomatized Shiveluch peridotite xenoliths contain high-Cr-number (>0·5) spinels (Figs 4a and 5a); they have inherited the mineral chemistry from their highly depleted dunite protoliths (Bryant *et al.*, 2007). The peridotite xenoliths from the SW Japan and NE Japan arcs are similar to abyssal peridotites in terms of spinel chemistry (Fig. 4b and c). The chromian spinels in some harzburgite xenoliths, especially those from Noyamadake and Vanuatu, have higher Mg-number at given Cr-numbers than the others (Fig. 5c and e). Chromian spinels in the high-Fe metasomatized peridotites from TUBAF plot off the olivine–spinel mantle array (Fig. 4e) and are relatively low in Mg-number (Fig. 5e). The Υ_{Fe} of chromian spinel is generally low, <0·1, except for metasomatized peridotites (Fig. 6a–e). Those peridotites that contain secondary hydrous minerals contain higher-Υ_{Fe} spinels than unmetasomatized ones in the Megata peridotite suite from the NE Japan arc (Abe *et al.*, 1992; Fig. 6b) and in the TUBAF peridotite suite from Papua New Guinea (Franz *et al.*, 2002; Fig. 6e).

The relationship between the Cr-number of chromian spinel, which is a good measure of the degree of depletion, and the Na content of the coexisting clinopyroxene, a possible measure of pressure of melting, can be used to characterize spinel peridotites (see Arai, 1991). Most of the Western Pacific peridotite xenoliths are characterized by the relatively low Na content of the clinopyroxene at a given Cr-number of the coexisting spinel (Fig. 7a–e). In some xenoliths, the Na contents are as low as those in abyssal peridotites (Fig. 7a–e), indicating relatively low pressures of equilibration. The peridotites from Noyamadake, SW Japan arc, as well as those from Oki-Dogo in the Sea of Japan off SW Honshu, contain high-Na clinopyroxenes at a given Cr-number of spinel (Fig. 7c). Almost all spinel peridotites from the Korean Peninsula, China and Sikhote-Alin (i.e. the current Eurasian continental margin) contain high-Na clinopyroxenes at a given Cr-number of spinel, plotting within the 'continental and hotspot' region of Fig. 7 (Arai *et al.*, 2007).

The secondary hydrous minerals (mainly pargasite and phlogopite) have relatively low Ti contents (Fig. 8a–d). They are lower in Ti content on average than their equivalents in the spinel peridotite xenoliths from NE China and Sikhote-Alin (Fig. 8a–d; Arai *et al.*, 2007). The Ti content in metasomatic amphiboles and phlogopites increases as a result of metasomatic fractionation of the involved agents (e.g. Arai & Takahashi, 1989). The low Ti content of the metasomatic amphiboles and phlogopite is characteristic of some of the mantle-wedge peridotites from the Western Pacific (Fig. 8a–d).

The peridotite xenoliths from the Takeshima seamount in the Sea of Japan (Fig. 1) can be classified into two types in terms of rare earth element (REE) characteristics of clinopyroxenes (Ninomiya *et al.*, 2007). Type 1 peridotites contain spinels of intermediate Cr-number, 0·4–0·5 (Fig. 4f), and clinopyroxenes with U-shaped REE distribution patterns. Type 2 peridotites contain spinels with slightly lower Cr-numbers (down to 0·3) (Fig. 4f) and clinopyroxenes with high REE contents and flat to light REE (LREE)-enriched REE patterns. The former are very similar to abyssal harzburgites in major-element mineral chemistry and middle (MREE) to heavy REE (HREE) contents of clinopyroxenes. In contrast, the latter are very similar to subcontinental lithospheric peridotites; for example, the xenoliths from China (Ninomiya *et al.*, 2007).

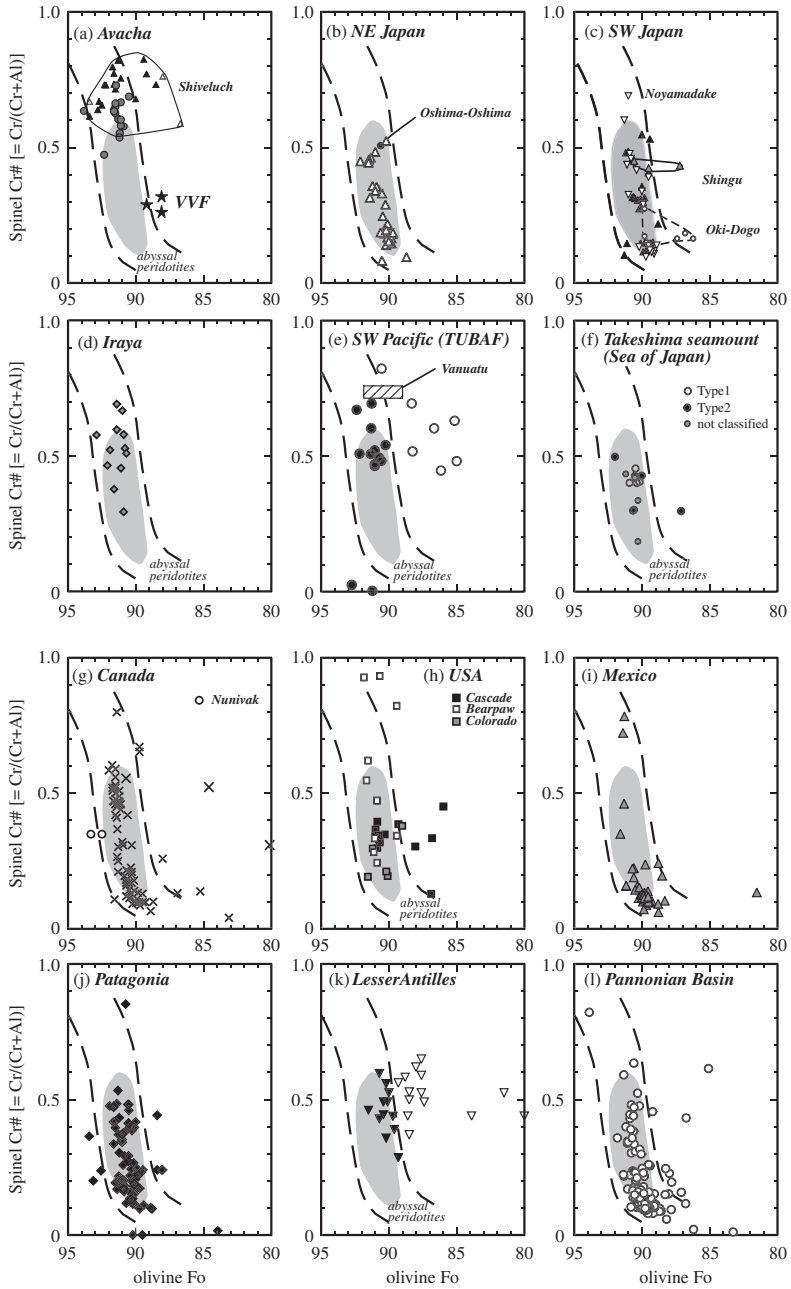

Fig. 4. Olivine–chromian spinel compositional relations in peridotite xenoliths from the mantle wedge. The field between the dashed lines is the olivine–spinel mantle array (OSMA) (Arai, 1994), which is a residual trend in the spinel peridotite stability field. The field (grey shaded) for abyssal peridotites (Arai, 1994) is shown for reference. (a) Avacha volcano, the Kamchatka arc. Data from Arai *et al.* (2003) and Ishimaru (2004). Peridotites from the Valovayam Volcanic Field (VVF) (Kepezhinskas *et al.*, 1995) and from Shiveluch volcano (Bryant *et al.*, 2007) are plotted for comparison. (b) NE Japan arc (Megata and Oshima-Oshima volcanoes). Data from Takahashi (1978*b*), Abe *et al.* (1992, 1995), Ninomiya & Arai (1992) and Abe (1997). (c) SW Japan arc. Data from Takahashi (1978*b*), Hirai (1986), Goto & Arai (1987) and Abe *et al.* (2003). (d) Iraya volcano, Batan Island, the Luzon–Taiwan arc. Data from Arai & Kida (2000) and Arai *et al.* (2004). (e) Southwestern Pacific (TUBAF seamount, the New Ireland arc, Papua New Guinea). Data from Franz & Wirth (2000), McInnes *et al.* (2001) and Franz *et al.* (2002). ○, Fe-rich peridotites that plot off the OSMA. Data for Merelava (Vanuatu) peridotites (Barsdell & Smith, 1989) are shown for comparison. (f) Sea of Japan (Takeshima seamount). Data from Ninomiya *et al.* (2007). The Takeshima peridotites are classified into Type 1 (back-arc basin type) and Type 2 (continental type). (g) Canadian Cordillera. Data from Francis (1987), Canil & Scarfe (1989), Shi *et al.* (1998), Peslier *et al.* (2002) and Harder & Russell (2006). Peridotites from Nunivak, western Alaska (Francis, 1976) are also plotted. (h) Western USA. Data from Draper (1992), Brandon & Draper (1996) and Ertan & Leeman (1996) for Cascades, from Riter & Smith (1996), Smith & Riter (1997) and Smith *et al.* (1999) for the Colorado Plateau, and from Downes *et al.* (2004) for Bearpaw. (i) Central Mexico. Data from Heinrich & Besch (1992), Luhr & Aranda-Gómez (1997) and Blatter & Carmichael (1998). (j) Patagonia. Data from Laurora *et al.* (2001), Rivalenti *et al.* (2004*a*, 2004*b*), Bjerg *et al.* (2005), and Schilling *et al.* (2005). (k) Lesser Antilles. Data from Parkinson *et al.* (2003). ∄, peridotites that plot off the OSMA. (l) Pannonian Basin, central Europe. Data from Downes *et al.* (1995), Konečný *et al.* (1995), Szabó *et al.* (1995), Vaselli *et al.* (1995), Dobosi *et al.* (1999) and Embey-Isztin *et al.* (2001).

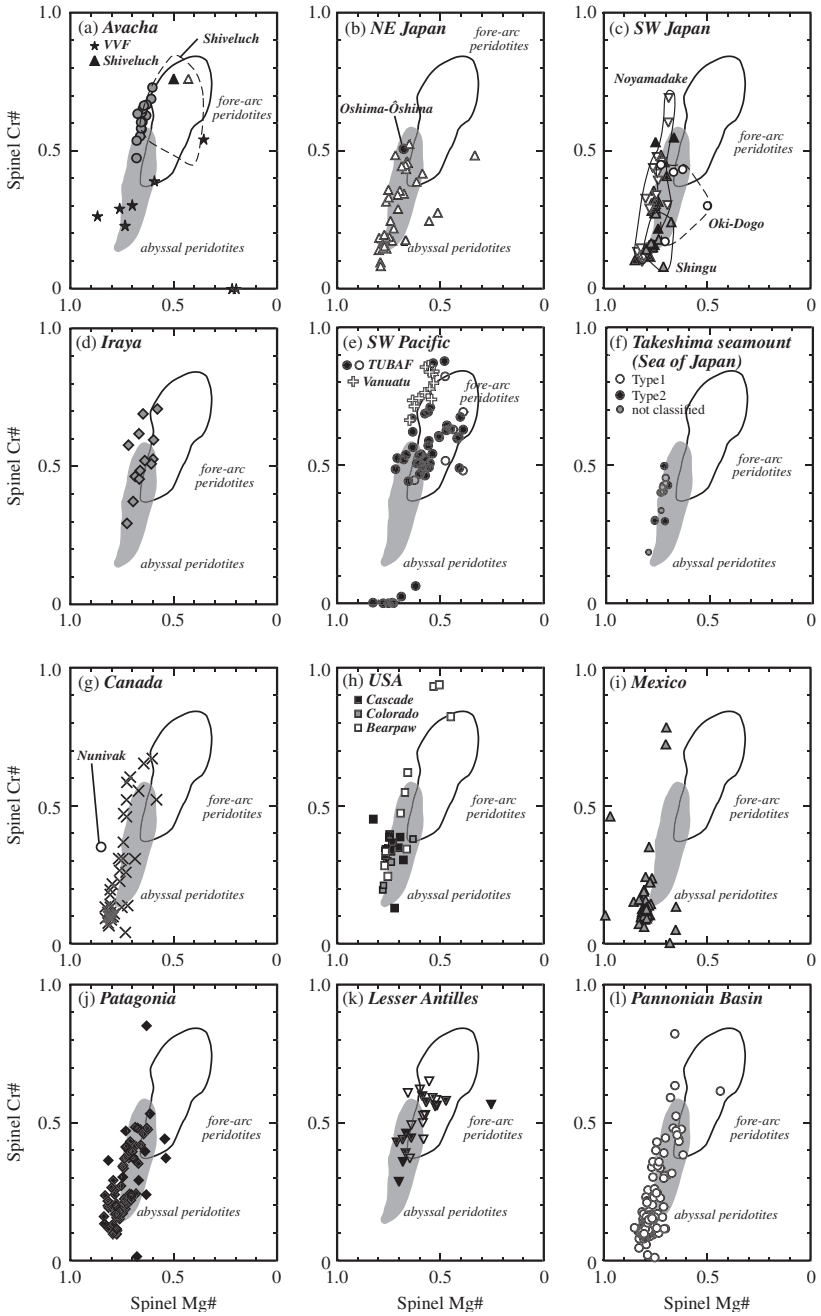

Fig. 5. Relationship between the Mg-number and Cr-number of chromian spinel in peridotite xenoliths from the mantle wedge. Field for abyssal peridotites (shaded) is after Dick & Bullen (1984). The fore-arc peridotite field is defined based on data from Bloomer & Hawkins (1983), Ishii (1985), Bloomer & Fisher (1987), Ishii *et al.* (1992, 2000), Pearce *et al.* (1992), Ohara & Ishii (1998), Parkinson & Pearce (1998), Pearce *et al.* (2000) and Okamura *et al.* (2006). (a) Avacha volcano, the Kamchatka arc. Data from Arai *et al.* (2003) and Ishimaru (2004). Peridotites from the Valovayam Volcanic Field (VVF) (Kepezhinskas *et al.*, 1995) and from Shiveluch volcano (Bryant *et al.*, 2007) are plotted for comparison. (b) NE Japan arc (Megata and Oshima-Ôshima volcanoes). Data from Takahashi (1978*b*), Abe *et al.* (1992, 1995), Ninomiya & Arai (1992) and Abe (1997). (c) SW Japan arc. Data from Takahashi (1978*b*), Hirai (1986), Goto & Arai (1987) and Abe *et al.* (2003). (d) Iraya volcano, Batan Island, the Luzon–Taiwan arc. Data from Arai & Kida (2000) and Arai *et al.* (2004). (e) Southwestern Pacific. Data for TUBAF seamount, the New Ireland arc, Papua New Guinea, are from Franz & Wirth (2000), McInnes *et al.* (2001) and Franz *et al.* (2002). Open symbol indicates Fe-rich peridotites that plot off the OSMA in Fig. 3e. Data for Merelava volcano, Vanuatu are from Barsdell & Smith (1989). (f) Sea of Japan (Takeshima seamount). Data from Ninomiya *et al.* (2007). The Takeshima peridotites are classified into Type 1 (back-arc basin type) and Type 2 (continental type). (g) Canadian Cordillera. Data from Francis (1987), Canil & Scarfe (1989), Shi *et al.* (1998) and Peslier *et al.* (2002). Peridotites from Nunivak, western Alaska (Francis, 1976*a*) are also plotted. (h) Western USA. Data from Draper (1992), Brandon & Draper (1996) and Ertan & Leeman (1996) for Cascades, from Riter & Smith (1996) and Smith *et al.* (1999) for the Colorado Plateau, and from Downes *et al.* (2004) for Bearpaw. (i) Central Mexico. Data from Heinrich & Besch (1992), Luhr & Aranda-Gómez (1997) and Blatter & Carmichael (1998). (j) Patagonia. Data from Laurora *et al.* (2001), Rivalenti *et al.* (2004*a*, 2004*b*), Bjerg *et al.* (2005) and Schilling *et al.* (2005). (k) Lesser Antilles. Data from Parkinson *et al.* (2003). Open symbols indicate Fe-rich peridotites that plot off the OSMA in Fig. 3j. (l) Pannonian Basin, central Europe. Data from Downes *et al.* (1995), Konečný *et al.* (1995), Szabó *et al.* (1995), Vaselli *et al.* (1995), Dobosi *et al.* (1999) and Embey-Isztin *et al.* (2001).

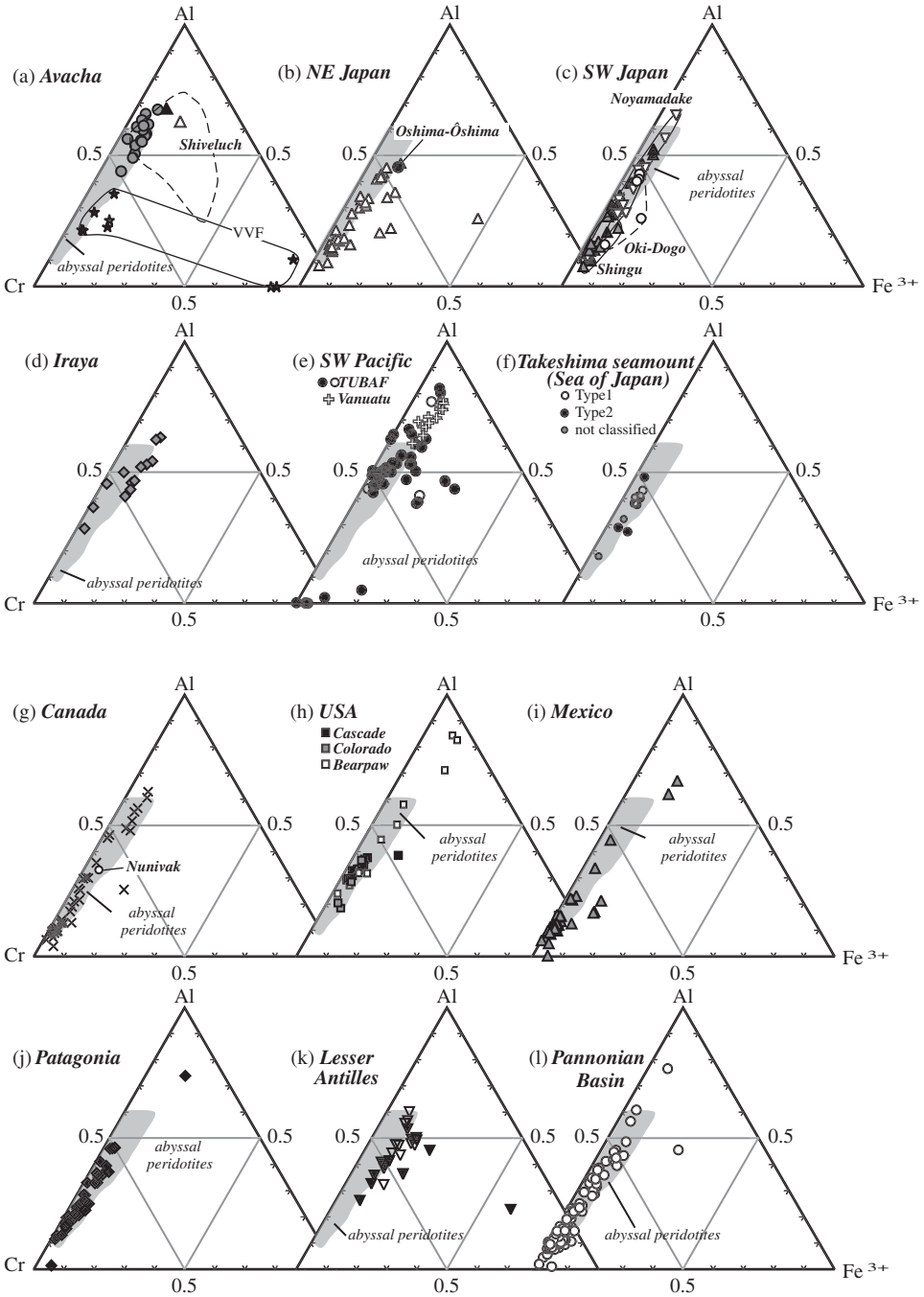

Fig. 6. Trivalent cation ratios in chromian spinel from peridotite xenoliths from the mantle wedge. Field for abyssal peridotites is from Arai *et al.* (2006*a*). Data sources and explanations are the same as in Fig. 4. (a) Avacha volcano, the Kamchatka arc. (b) NE Japan arc (Megata and Oshima-Ôshima volcanoes). (c) SW Japan arc. (d) Iraya volcano, Batan Island, the Luzon–Taiwan arc. (e) Southwestern Pacific (TUBAF seamount, the New Ireland arc, Papua New Guinea and Merelava, Vanuatu). (f) Sea of Japan (Takeshima seamount). (g) Canadian Cordillera. (h) Western USA. (i) Central Mexico. (j) Patagonia. (k) Lesser Antilles. (l) Pannonian Basin, central Europe.

Equilibrium conditions

It is difficult to estimate equilibration pressures for spinel peridotites because of the lack of an appropriate geobarometer. Fertile low-Cr/Al peridotites are characterized by spinel lherzolite mineral assemblages, with or without plagioclase, indicating their derivation within or at the low-pressure limit of the spinel lherzolite stability field. The peridotite xenoliths from the Western Pacific arcs are

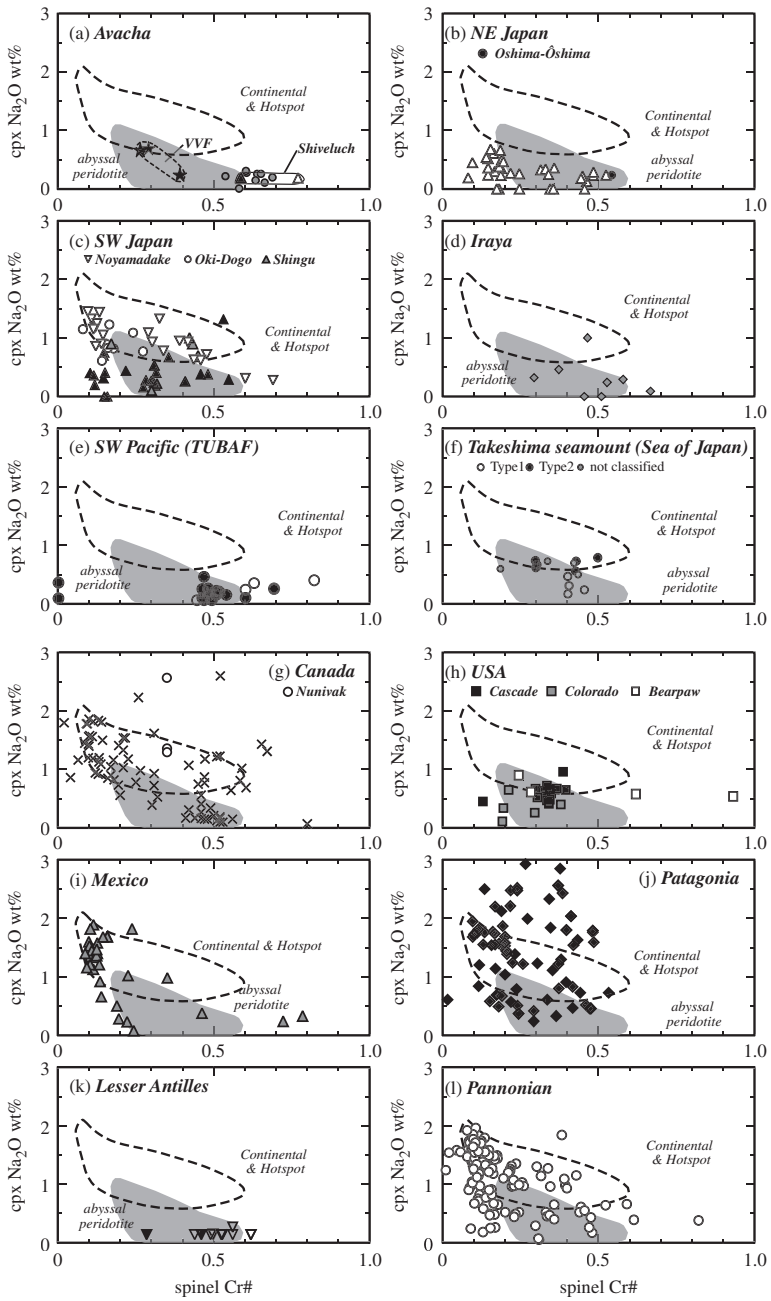

Fig. 7. Relationships between the Na_2O content of clinopyroxene and the Cr-number of chromian spinel in peridotite xenoliths from the mantle wedge. Fields for continental and hotspot peridotites and abyssal peridotite are after Arai (1991). (a) Avacha volcano, the Kamchatka arc. Data from Arai *et al.* (2003) and Ishimaru (2004). Peridotites from the Valovayam Volcanic Field (VVF) (Kepezhinskas *et al.*, 1995) and from Shiveluch volcano (Bryant *et al.*, 2007) are plotted for comparison. (b) NE Japan arc (Megata and Oshima-Ôshima volcanoes). Data from Takahashi (1978*b*), Abe *et al.* (1992, 1995, 1998), Ninomiya & Arai (1992) and Abe (1997). (c) SW Japan arc. Data from Takahashi (1978*b*), Hirai (1986), Goto & Arai (1987) and Abe *et al.* (2003). (d) Iraya volcano, Batan Island, the Luzon–Taiwan arc. Data from Arai & Kida (2000) and Arai *et al.* (2004). (e) Southwestern Pacific (TUBAF seamount, the New Ireland arc, Papua New Guinea). Data from Franz & Wirth (2000), McInnes *et al.* (2001) and Franz *et al.* (2002). Open symbol indicates Fe-rich peridotites that plot off the OSMA in Fig. 3e. (f) Sea of Japan (Takeshima seamount). Data from Ninomiya *et al.* (2007). The Takeshima peridotites are classified into Type 1 (back-arc basin type) and Type 2 (continental type). (g) Canadian Cordillera. Data from Francis (1987), Canil & Scarfe (1989), Shi *et al.* (1998), Peslier *et al.* (2002) and Harder & Russell (2006). Peridotites from Nunivak, western Alaska (Francis, 1976) are also plotted. (h) Western USA. Data from Draper (1992) and Brandon & Draper (1996) for Cascades, from Riter & Smith (1996) and Smith *et al.* (1999) for the Colorado Plateau, and from Downes *et al.* (2004) for Bearpaw. (i) Central Mexico. Data from Luhr & Aranda-Gómez (1997) and Blatter & Carmichael (1998). (j) Patagonia. Data from Laurora *et al.* (2001), Rivalenti *et al.* (2004*a*, 2004*b*), Bjerg *et al.* (2005) and Schilling *et al.* (2005). (k) Lesser Antilles. Data from Parkinson *et al.* (2003). Open symbols indicate Fe-rich peridotites that plot off the OSMA in Fig. 3j. (l) Pannonian Basin, central Europe. Data from Downes *et al.* (1995), Konečný *et al.* (1995), Szabó *et al.* (1995), Vaselli *et al.* (1995), Embey-Isztin *et al.* (2001) and Bali *et al.* (2002).

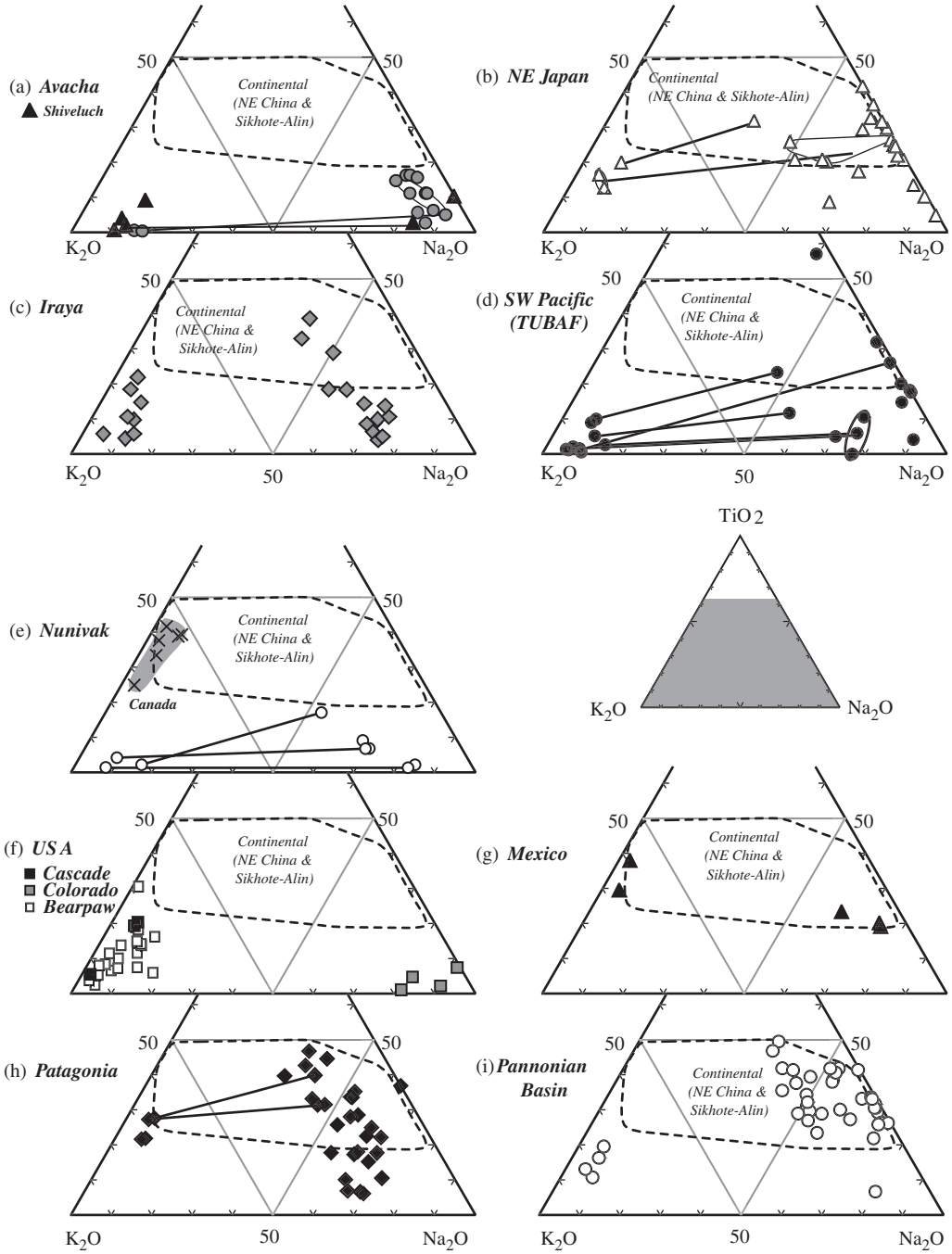

Fig. 8. TiO_2–K_2O–Na_2O weight ratios of hydrous minerals in peridotite xenoliths from the mantle wedge. Amphiboles and phlogopites plot in the Na-rich and K-rich parts of the diagram, respectively. Field for hydrous minerals in sub-continental peridotite xenoliths from NE China and Sikhote-Alin is shown by a dotted line (Arai *et al.*, 2007). (a) Avacha and Shiveluch volcanoes, the Kamchatka arc. Data from Ishimaru (2004), Bryant *et al.* (2007) and Ishimaru *et al.* (2007). (b) NE Japan arc (Megata volcano). Data from Arai (1986), Goto & Arai (1987), Abe *et al.* (1992, 1995) and Abe (1997). (c) Iraya volcano, Batan Island, the Luzon–Taiwan arc. Data from Kida (1998). (d) Southwestern Pacific (TUBAF seamount, the New Ireland arc, Papua New Guinea). Data from McInnes *et al.* (2001) and Franz *et al.* (2002). (e) Nunivak, west Alaska Francis (1976) and Kostal Lake, the Canadian Cordillera (Canil & Scarfe, 1989). (f) Western USA. Data from Draper (1992) and Ertan & Leeman (1996) for Cascades, from Smith (1979) and Smith *et al.* (1999) for the Colorado Plateau, and from Downes *et al.* (2004) for Bearpaw. (g) Central Mexico. Data from Luhr & Aranda-Gómez (1997) and Blatter & Carmichael (1998). (h) Patagonia. Data from Gorring & Kay (2000), Laurora *et al.* (2001), Rivalenti *et al.* (2004*a*, 2004*b*) and Bjerg *et al.* (2005). (i) Pannonian Basin, central Europe. Data from Szabó *et al.* (1995), Vaselli *et al.* (1995) and Zanetti *et al.* (1995).

characterized by relatively low two-pyroxene equilibration temperatures calculated using the two-pyroxene thermomoter of Wells (1977), except for those from the SW Japan arc (Fig. 9a–e). As pointed out by Takahashi (1978*a*), the peridotite xenoliths from the SW Japan arc exhibit higher equilibrium temperatures than those from the NE Japan arc (Fig. 9b and c). Some of the SW Japan arc peridotites, especially those from Noyamadake, exhibit extremely high temperatures, around 1200°C on average (Fig. 9c). The relatively high Mg-number of chromian spinels at given Cr-numbers in the Noyamadake and Vanuatu harzburgites (Fig. 5c and e) are partly due to their high equilibeium temperatures (Fig. 9).

Oxygen fugacity

The olivine–orthopyroxene–spinel oxygen barometer (Ballhaus *et al.*, 1990) was used to estimate the oxidation state recorded by the Western Pacific mantle-wedge peridotite xenoliths, assuming a 1·5 GPa equilibrium pressure (Fig. 10). The majority of the peridotite xenoliths from the Kamchatka, Luzon–Taiwan (Iraya volcano) and NE Japan arcs have relatively high oxygen fugacities, $\triangle \log (fO_2)_{FMQ} > 0$, where $\triangle \log (fO_2)_{FMQ}$ is a log unit difference in oxygen fugacity from the fayalite–magnetite–quartz buffer. In contrast to this, the peridotite xenoliths from the SW Japan arc exhibit almost the same range of $\triangle \log (fO_2)_{FMQ}$ as abyssal peridotites (Ballhaus *et al.*, 1991). The peridotite xenoliths from Avacha, Shiveluch and TUBAF, which are metasomotized to various degrees (e.g. Franz *et al.*, 2002; Bryant *et al.*, 2007; Ishimaru *et al.*, 2007), display especially high oxidation states (Fig. 10a and e). The mantle wedge of the Western Pacific has oxygen fugacity equal to or slightly higher than that of the abyssal mantle (Fig. 10a–e), consistent with the result of Parkinson & Arculus (1999).

PETROLOGICAL CHARACTERISTICS OF PERIDOTITE XENOLITHS FROM OTHER ARCS

It is useful to compare the characteristics of the Western Pacific mantle-wedge peridotites with those from other arcs to obtain a general overview of the petrological characteristics of the mantle wedge. It is also possible to evaluate the 'maturity' of the mantle wedge because some of the Western Pacific peridotites are derived from well-established mature subduction systems. We did not consider the mineral chemistry of garnet-bearing ultramafic rocks because we have found no equivalents within the Western Pacific arcs to compare with.

Western North America

Western Alaska

Several mantle xenolith localities are known from western Alaska, within the back-arc region of the eastern end of the Aleutian arc (e.g. Swanson *et al.*, 1987). Nunivak Island in the Bering Sea off western Alaska is the most famous of these (e.g. Francis, 1976*a*, 1976*b*; Swanson *et al.*, 1987). Amphibole-bearing pyroxenite and peridotite xenoliths have been reported from Nunivak (Francis, 1976*a*, 1976*b*). The relatively high Fo content of olivine and Cr-number of spinel (Figs 4g, 5g and 6g) may indicate the predominance of harzburgite. Clinopyroxenes are relatively high in Na at an intermediate Cr-number of spinel (Fig. 7g), suggesting metasomatic modification. The most prominent characteristic of the Nunivak peridotite xenoliths is the low Ti content of the hydrous minerals (Fig. 8e). This feature is common to the mantle-wedge peridotite xenoliths from the Avacha and Shiveluch (Kamchatka arc), Iraya (Luzon–Taiwan arc) and TUBAF (New Ireland arc, Papua New Guinea) volcanoes (Fig. 8a–d). The Nunivak peridotites display relatively high oxygen fugacities, slightly higher than the FMQ buffer (Fig. 10g).

Canadian Cordillera, British Columbia

Numerous mantle xenolith localities have been reported from the western part of Canada (e.g. British Columbia; Mitchell, 1987; Shi *et al.*, 1998; Peslier *et al.*, 2002), which was a convergent continental margin during the Phanerozoic (e.g. Peslier *et al.*, 2002). Some of the high-temperature (1000–1100°C) harzburgite xenoliths from the northern Cordillera have been considered to be representative of asthenospheric mantle materials rising through a slab window (Shi *et al.*, 1998). The lithology of the peridotites is variable from fertile lherzolite to depleted harzburgite (Fig. 3f) (Littlejohn & Greenwood, 1974; Fujii & Scarfe, 1982; Brearley *et al.*, 1984; Francis, 1987; Shi *et al.*, 1998; Peslier *et al.*, 2002; Harder & Russell, 2006). Wehrlite and wehrlitic lherzolite are also common (Peslier *et al.*, 2002). The Canadian Cordilleran peridotite xenoliths are almost anhydrous; no hydrous minerals have been documented except for phlogopite-bearing peridotite xenoliths from Kostal Lake (Canil & Scarfe, 1989). Most of the lherzolite to harzburgite xenoliths from the Canadian Cordillera plot in the abyssal peridotite field in terms of mode (Fig. 3f) and Fo (olivine)–Cr-number (spinel) compositions (Fig. 4g). The Mg-number of spinel in the peridotites is slightly higher in the Canadian Cordillera than in the present-day ocean floor at a given Cr-number, consistent with the high-temperature conditions of equilibration (e.g. Shi *et al.*, 1998) (Fig. 5g). The Υ_{Fe} of the spinel is notably low, <0·1 (Fig. 6g). The Na content of clinopyroxene decreases sharply with an increase in the Cr-number of the coexisting chromian

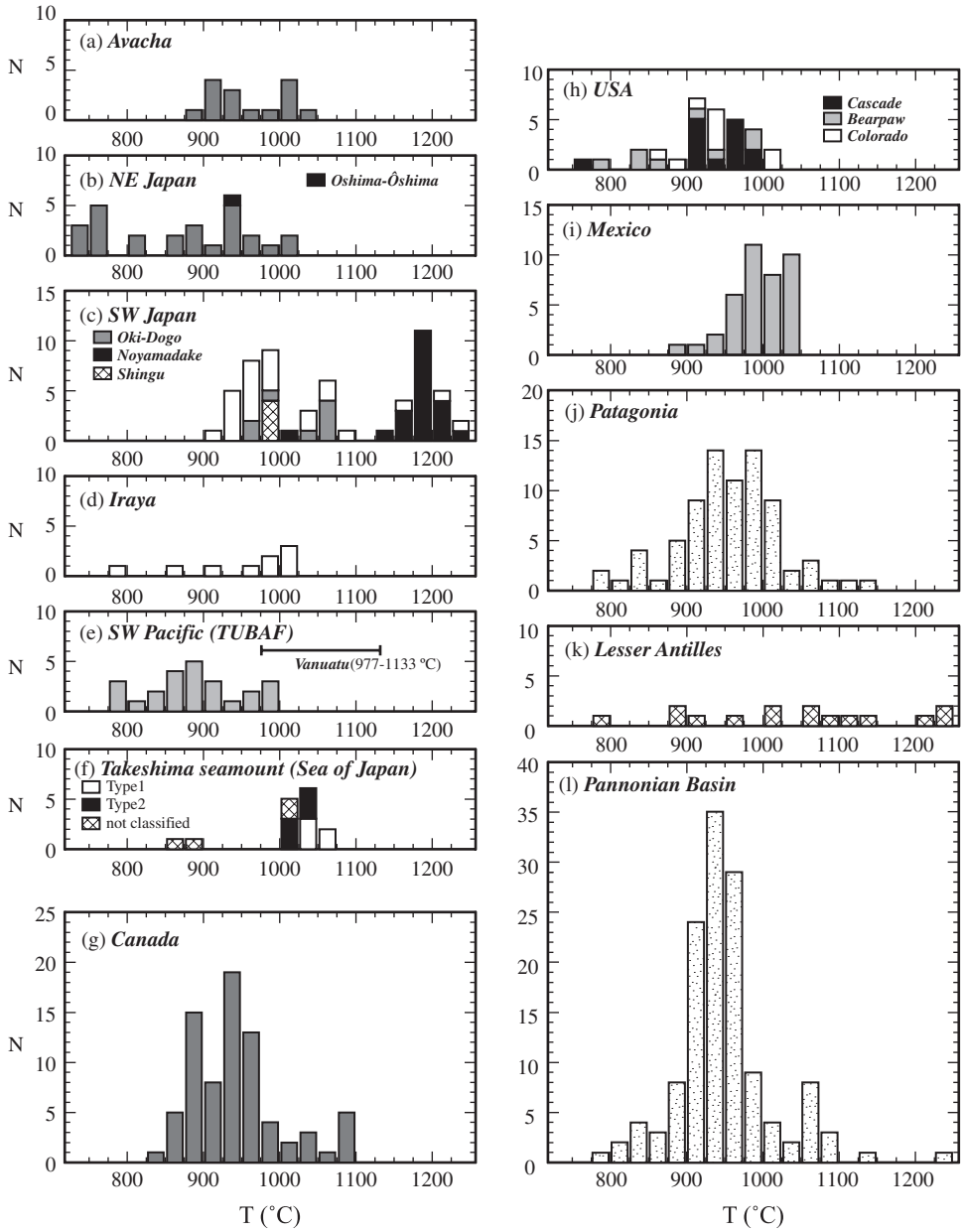

Fig. 9. Histograms of the calculated equilibrium temperature in peridotite xenoliths from the mantle wedge. The two-pyroxene thermometer of Wells (1977) was used. (a) Avacha volcano, the Kamchakta arc. Data from Arai *et al.* (2003) and Ishimaru *et al.* (2007). (b) NE Japan arc. Data from Takahashi (1978*b*), Abe *et al.* (1992), Ninomiya & Arai (1992) and Abe (1997). (c) SW Japan arc. Data from Takahashi (1978*b*), Hirai (1986), Goto & Arai (1987) and Abe *et al.* (2003). (d) Iraya volcano, the Luzon–Taiwan arc. Data from Arai & Kida (2000) and Arai *et al.* (2004). (e) Southwestern Pacific (TUBAF seamount, the New Ireland arc, Papua New Guinea). Data from McInnes *et al.* (2001) and Franz *et al.* (2002). Only the range is shown for Merelava peridotite, Vanuatu (Barsdell & Smith, 1989). (f) Sea of Japan (Takeshima seamount). Data from Ninomiya *et al.* (2007). The Takeshima peridotites are classified into Type 1 (back-arc basin type) and Type 2 (continental type). (g) Canadian Cordillera. Data from Francis (1987), Canil & Scarfe (1989), Shi *et al.* (1998), Peslier *et al.* (2002) and Harder & Russell (2006). (h) Western USA. Data from Draper (1992), Brandon & Draper (1996) and Ducea & Saleeby (1998) for Cascades and Sierra Nevada, from Riter & Smith (1996), Smith & Riter (1997) and Smith *et al.* (1999) for the Colorado Plateau, and from Downes *et al.* (2004) for Bearpaw. (i) Central Mexico. Data from Heinrich & Besch (1992), Luhr & Aranda-Gómez (1997) and Blatter & Carmichael (1998). (j) Patagonia. Data from Gorring & Kay (2000), Laurora *et al.* (2001), Kilian & Stern (2002), Rivalenti *et al.* (2004*a*, 2004*b*), Bjerg *et al.* (2005) and Schilling *et al.* (2005). (k) Lesser Antilles. Data from Parkinson *et al.* (2003). (l) Pannonian Basin, central Europe. Data from Szabó & Taylor (1994), Downes *et al.* (1995), Konečný *et al.* (1995), Szabó *et al.* (1995), Vaselli *et al.* (1995), Dobosi *et al.* (1999) and Embey-Isztin *et al.* (2001).

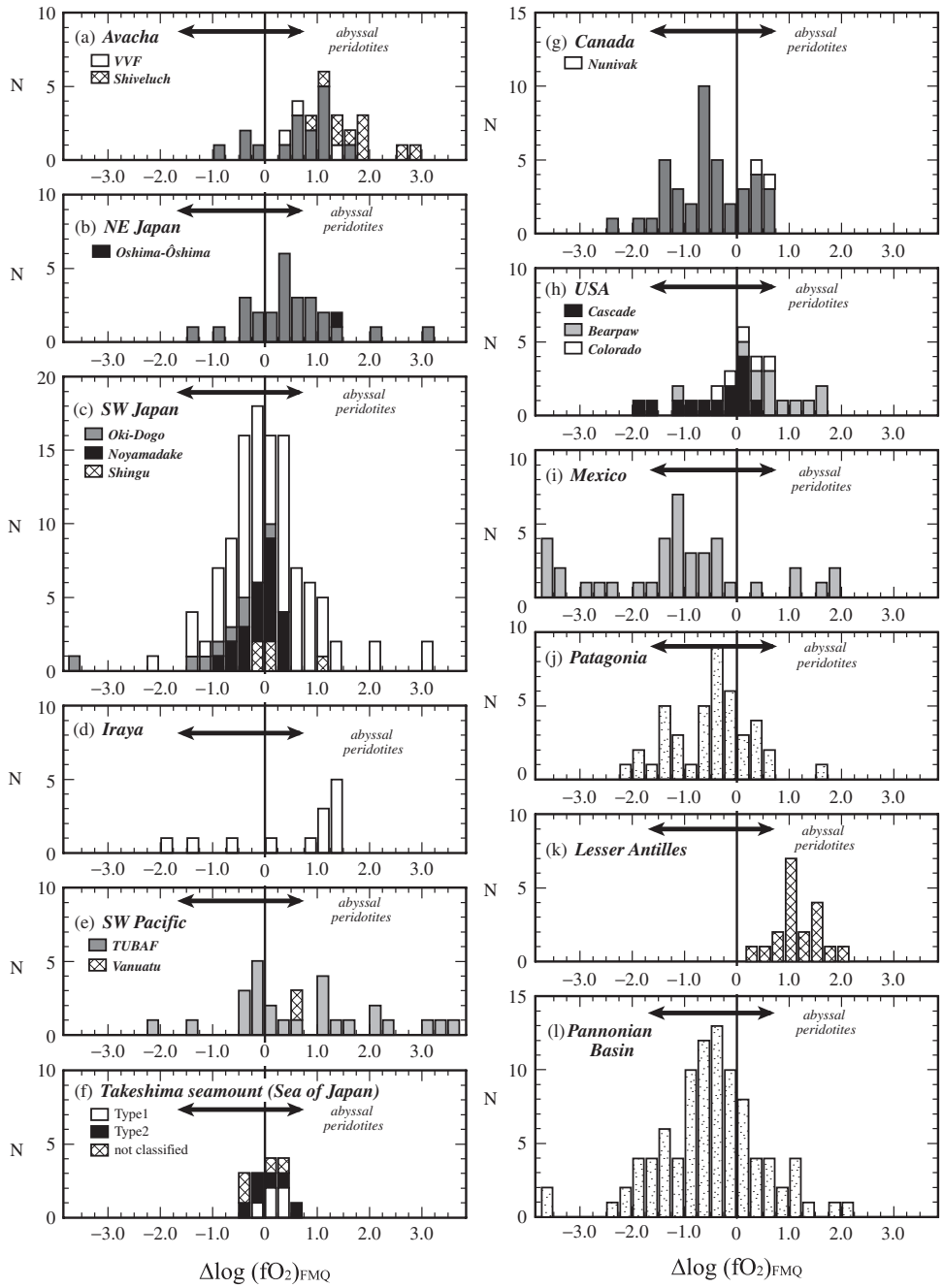

Fig. 10. Histograms of the calculated oxygen fugacity relative to the fayalite–magnetite–quartz buffer. Oxygen geobarometry after Ballhaus *et al.* (1991), assuming a pressure of 1·5 GPa. (a) Kamchatka arc (Avacha and Shiveluch volcanoes and the Valovayam Volcanic Field (VVF)). Data from Kepezhinskas *et al.* (1995), Arai *et al.* (2003), Bryant *et al.* (2007) and Ishimaru *et al.* (2007). (b) NE Japan arc. Data from Takahashi (1978*b*), Ninomiya & Arai (1992), Abe *et al.* (1992) and Abe (1997). (c) SW Japan arc. Data from Takahashi (1978*b*), Hirai (1986), Goto & Arai (1987) and Abe *et al.* (2003). (d) Iraya volcano, the Luzon–Taiwan arc. Data from Arai & Kida (2000) and Arai *et al.* (2004). (e) Southwestern Pacific (TUBAF seamount, the New Ireland arc, Papua New Guinea, and Merelava volcano, Vanuatu). Data from Barsdell & Smith (1989), Franz & Wirth (2000), McInnes *et al.* (2001) and Franz *et al.* (2002). (f) Sea of Japan (Takeshima seamount). Data from Ninomiya *et al.* (2007). The Takeshima peridotites are classified into Type 1 (back-arc basin type) and Type 2 (continental type). (g) Canadian Cordillera. Nunivak xenoliths (Francis, 1976), western Alaska, are shown here. Data from Francis (1987), Canil & Scarfe (1989), Shi *et al.* (1998) and Peslier *et al.* (2002). (h) Western USA. Data from Draper (1992) and Brandon & Draper (1996) for Cascades, from Riter & Smith (1996) and Smith *et al.* (1999) for the Colorado Plateau, and from Downes *et al.* (2004) for Bearpaw. (i) Central Mexico. Data from Heinrich & Besch (1992), Luhr & Aranda-Gómez (1997) and Blatter & Carmichael (1998). (j) Patagonia. Data from Laurora *et al.* (2001), Rivalenti *et al.* (2004*b*), Bjerg *et al.* (2005) and Schilling *et al.* (2005). (k) Lesser Antilles. Data from Parkinson *et al.* (2003). (l) Pannonian Basin, central Europe. Data from Szabó & Taylor (1994), Downes *et al.* (1995), Konečný *et al.* (1995), Szabó *et al.* (1995), Vaselli *et al.* (1995), and Dobosi *et al.* (1999).

spinel (Fig. 7g). Generally, the lherzolites plot in the continental-rift zone–oceanic hotspot peridotite field, whereas some of the harzburgites plot in the abyssal peridotite field (Fig. 7g). The phlogopite from Kostal Lake (Canil & Scarfe, 1989) is rich in Ti compared with phlogopites from other mantle-wedge peridotite xenoliths (Fig. 8). Calculated equilibrium temperatures vary from <900 to 1100°C (mostly from 900–1000°C) (Fig. 9g). The calculated oxygen fugacity is relatively low, being equivalent to or lower than the FMQ buffer (Fig. 10g).

Cascade Range to Sierra Nevada

The region from the Cascade Range, Washington, to the Sierra Nevada, California, which forms part of the Mesozoic–Cenozoic convergent margin of the North American continent, provides plenty of ultramafic xenolith localities including material possibly derived from the mantle wedge (e.g. Draper, 1992; Brandon & Draper, 1996; Ertan & Leeman, 1996; Ducea & Saleeby, 1998). The host volcanic rocks are alkali basalts and related rocks of Plio-Pleistocene age (Draper, 1992; Ducea & Saleeby, 1998). Xenoliths from Simcoe, Washington, are considered to be representative of the mantle wedge beneath the Cascade arc, and have been the most extensively studied (Draper, 1992; Brandon & Draper, 1996; Ertan & Leeman, 1996). Lherzolitic harzburgite to harzburgite is predominant (Fig. 3g) and contains intermediate Cr-number (mostly around 0·2–0·5) chromian spinel (Figs 4g, 5g and 6g). Some xenolith olivines have relatively low Fo contents (down to 86) (Fig. 4h), possibly as a result of secondary metasomatism, which produced both orthopyroxene and phlogopite (Ertan & Leeman, 1996). The chromian spinel falls almost entirely within the abyssal peridotite field, except for one analysis from a phlogopite-bearing olivine orthopyroxenite, the end product of the metasomatism (Ertan & Leeman, 1996) (Fig. 5h). The Na content of the clinopyroxene is relatively low. The Simcoe peridotites plot around the boundary between the abyssal peridotite and continental-rift zone–hotspot peridotite fields in terms of their Na (clinopyroxene)–Cr-number (spinel) relationships (Fig. 7h). Metasomatic phlogopite in some Simcoe peridotites (Ertan & Leeman, 1996) is low in Ti (Fig. 8f). Calculated temperatures are lower than 1000°C (Fig. 9h), and oxygen fugacity values are mostly around the FMQ buffer or lower (Fig. 10h).

Colorado Plateau

The Colorado Plateau and surrounding region, southwestern USA, is known for its numerous mantle-derived ultramafic xenolith localities (e.g. Menzies *et al.*, 1987). Although the link with subduction is more tenuous compared with the other localities mentioned thus far, the deep-seated xenoliths from the Colorado Plateau have been used to provide information about the role of subduction processes in the evolution of the sub-cratonic mantle (e.g. Alibert, 1994; Riter & Smith, 1996; Smith & Riter, 1997; Smith *et al.*, 1999; Smith, 2000). The host-rocks are alkali basalts of Tertiary age within the Plateau margins and kimberlites or minettes of Quaternary age in the Navajo volcanic field (e.g. Ehrenberg, 1979; Alibert, 1994).

Anhydrous lherzolites predominate (Fig. 3g); these contain chromian spinels with low to intermediate Cr-numbers (mostly 0·2–0·4) (Figs 4h and 5h; Alibert, 1994). Some are garnet-bearing lherzolites with phlogopite (e.g. The Thumb; Ehrenberg, 1979, 1982); others are strongly hydrated peridotites, containing antigorite, chlorite, amphibole and titanoclinohumite (Green Knobs and Buell Park; Smith, 1979). Some of the peridotites from the Grand Canyon at the western margin of the Plateau are slightly hydrous and characterized by low-Al orthopyroxene (Smith & Riter, 1997; Smith *et al.*, 1999; Smith, 2000). Chromian spinel from the Colorado Plateau peridotites falls within the range of abyssal peridotite spinels except for one analysis (Figs 5h and 6h). The Na content of clinopyroxene is characteristically low in the Colorado Plateau peridotites (Fig. 7h). Amphibole is very low in Ti (Fig. 8h). Temperatures calculated are mostly lower than 1000°C (Fig. 9h). The oxygen barometer yields oxygen fugacities around the FMQ buffer (Fig. 10h).

Bearpaw Mountains, Montana

The peridotite xenolith suite from the Bearpaw Mountains, Montana, USA (Downes *et al.*, 2004), is exceptional: the locality lies within the Wyoming craton, far from any current or recent subduction zones. The peridotite xenoliths, however, have been interpreted to reflect supra-subduction zone metasomatism, possibly of Cretaceous age (Downes *et al.*, 2004).

The Bearpaw xenoliths, exhumed by a minette with an age of 50–54 Ma, comprise tectonites of depleted harzburgite, lherzolite and dunite, associated with cumulative rocks (wehrlites and pyroxenites) (Fig. 3g; Downes *et al.*, 2004). Only the tectonites (mantle peridotites) are considered here. The peridotites exhibit metasomatic textures, including the growth of phlogopite and orthopyroxene (the 'white orthopyroxene') to various extents (Downes *et al.*, 2004). The Cr-number of chromian spinel is highly variable from 0·2 to >0·9 (Figs 4h, 5h and 6h) at a rather constant Fo content of olivine (around 91) (Fig. 4h). The Na content of clinopyroxene is relatively low, <1 wt% of Na_2O (Fig. 7h). The secondary phlogopite is characterized by low Ti contents (Fig. 8f), equivalent to those of the Iraya xenoliths (Fig. 8c). The Bearpaw peridotites display equilibrium temperatures lower than 1000°C (Fig. 9h), and oxygen fugacity values higher than the FMQ buffer (Fig. 10h). The estimated age of the depleted peridotite protolith is very old (Proterozoic), and the tectonic setting of the melting is not clear (Downes *et al.*, 2004). The depleted peridotite xenoliths from Bearpaw Mountains are similar to

some mantle-wedge peridotites from the Western Pacific (e.g. Fig. 3), although the degree of melting may be higher for the former.

Central Mexico

Quaternary alkali basalts in central Mexico host peridotite xenoliths (Arand-Gómez & Ortega-Gutiérrez, 1987) assumed to be derived from the mantle wedge and back-arc mantle (e.g. Heinrich & Besch, 1992; Luhr & Aranda-Gómez, 1997). Several xenolith localities provide a transect oblique to the paleo-trench during the Mesozoic–Tertiary, along which the Farallon plate was subducted eastward (Luhr & Aranda-Gómez, 1997). One hornblende andesite of arc affinity from El Peñon, central Mexico, includes hydrous ultramafic xenoliths derived from the mantle wedge (Blatter & Carmichael, 1998). Lherzolites are predominant over harzburgites in terms of mode and mineral chemistry (Figs 3h and 4i) (Heinrich & Besch, 1992; Luhr & Aranda-Gómez, 1997; Blatter & Carmichael, 1998). Olivine-bearing websterites from El Peñon contain high-Cr-number (0·7–0·8) chromian spinels (Figs 4i, 5i and 6i). The lherzolites contain high-Na clinopyroxenes associated with low-Cr-number spinels (Fig. 7i). Along the transect across the palaeo-arc in central Mexico, hydrous peridotite was found only at the easternmost xenolith locality (Ventura–Espíritu Santo); its phlogopite is high in Ti relative to alkalis (Na + K) (Fig. 8g). Calculated equilibrium temperatures are around 1000°C (Fig. 9i). The peridotite xenoliths from the transect have low oxygen fugacities [$\Delta\log (fO_2)_{FMQ} < 0$] (Fig. 10i), which, however, increase westward approaching the location of the Mesozoic palaeo-trench (Luhr & Aranda-Gómez, 1997). The westward increase in oxygen fugacity has been related to an increase in the effects of the underlying slab during the Mesozoic (Luhr & Aranda-Gómez, 1997). The El Peñon hydrous peridotites, which may be derived from the present-day mantle wedge above the northerly subducting Cocos plate, display remarkably high oxygen fugacity values [$\Delta\log (fO_2)_{FMQ}$ up to two] (Fig. 10i; Blatter & Carmichael, 1998).

Patagonia

The western margin of the South American continent forms part of the Andean subduction system (e.g. Dewey & Lamb, 1992; Ramos, 1999). Ultramafic xenoliths entrained within Cenozoic volcanic rocks occur at widely distributed localities within the Northern, Southern and Austral Volcanic Zones of the Andean arc (e.g. Conceição *et al.*, 2005), in addition to several famous localities of subcratonic mantle xenoliths entrained by kimberlitic rocks in Brazil (e.g. Meyer & Svisero, 1987). A variety of garnet-bearing pyroxenite xenoliths has been described from andesites in the Mercaderes region of the Northern Volcanic Zone, Colombia (e.g. Rodriguez-Vargas *et al.*, 2005). Late Cretaceous basanites erupted along a rift zone (at the edge of the Cenozoic Andean plateau) of the same age inland of the Central Volcanic Zone entrain spinel peridotite and pyroxenite xenoliths (Lucassen *et al.*, 2005). The xenoliths are mainly lherzolites, in which the Cr-number of spinel ranges from 0·1 to 0·5 (mainly 0·1–0·3) (Lucassen *et al.*, 2005). The equilibrium temperature of the Cretaceous xenoliths ranges from 900 to 1100°C (Lucassen *et al.*, 2005).

Patagonia forms the southern tip of the South American continent within the back-arc region of the Southern and Austral Volcanic Zones and has numerous mantle xenolith localities (Ramos *et al.*, 1982). The Southern and Austral Volcanic Zones lie above the Nazca plate and the Antarctic plate, respectively, which are subducting east-northeastward (e.g. Ramos & Kay, 1992). Behind the Andean volcanic arc, large volumes of 'plateau lavas' have erupted since the late Cretaceous (e.g. Stern *et al.*, 1990). The petrogenesis of the Pliocene–Quaternary alkali basalts has been explained in terms of slab window formation after the collision of the Nazca–Antarctica ridge (e.g. Gorring & Kay, 2001); these basalts exhume xenoliths from the Panagonian mantle (e.g. Ramos *et al.*, 1982; Rivalenti *et al.*, 2004*a*; Bjerg *et al.*, 2005). Most of the peridotite xenoliths are of spinel lherzolite and harzburgite, except for two localities of garnet peridotite (Pali Aike and Prahuaniyeu) (e.g. Stern *et al.*, 1999; Bjerg *et al.*, 2005). Peridotite xenoliths from Gobernador Gregores (Laurora *et al.*, 2001; Rivalenti *et al.*, 2004*a*, 2004*b*; Bjerg *et al.*, 2005) are exceptionally hydrated, containing up to 7 vol. % of pargasitic amphibole and a trace amount of phlogopite (e.g. Rivalenti *et al.*, 2004*a*, 2004*b*). The presence of wehrlite or wehrlitic lherzolite is noteworthy (Rivalenti *et al.*, 2004*a*, 2004*b*; Fig. 3i).

The Patagonian peridotites are similar to abyssal peridotites in mode and major-element mineral chemistry (Figs 3i, 4j, 5j and 6j). Some spinels are exceptionally high (>0·8) or low (nearly zero) in Cr-number (Figs 4i, 5i and 6i). Lithologically the xenoliths vary from fertile lherzolite to relatively depleted harzburgite, lherzolite being slightly predominant over harzburgite (e.g. Fig. 4i). Amphibole and phlogopite vary from low-Ti to high-Ti varieties (Fig. 8h), and are similar in chemistry to equivalent lithologies from the Western Pacific arcs; for example, Megata (NE Japan arc) (Fig. 8b) and Iraya (Luzon–Taiwan arc) (Fig. 8c). The most prominent feature of the mineral chemistry of the Patagonian peridotites is the relatively high content of Na_2O, up to 3 wt % (e.g. Gorring & Kay, 2000; Rivalenti *et al.*, 2004*a*, 2004*b*), in the clinopyroxene (Fig. 7j). Some of the high-Na clinopyroxenes are also rich in Cr_2O_3, up to >2 wt % (Rivalenti *et al.*, 2004*b*), suggesting the incorporation of a kosmochlor component ($NaCrSi_2O_6$) (see Ikehata & Arai, 2004).

The presence of kosmochlor-bearing diopside suggests that carbonatite metasomatism has occurred within the mantle beneath Patagonia (Yaxley *et al.*, 1991; Yaxley & Green, 1996; Ikehata & Arai, 2004). Other lines of petrographic (wehrlite occurrence) and geochemical [high field strength element (HFSE) depletion] evidence also suggest the occurrence of carbonatite metasomatism (e.g. Gorring & Kay, 2000; Laurora *et al.*, 2001; Rivalenti *et al.*, 2004*b*). The Patagonian peridotites could represent residual peridotites formed by back-arc extension contemporaneous with the plateau basalt phase of magmatism. Several stages of metasomatism (e.g. Gorring & Kay, 2000), including the carbonatite metasomatism, may have been related to asthenospheric upwelling through a slab window (e.g. Gorring & Kay, 2001). The effects of the current subduction of the Nazca and Antarctic plates are not clear from the peridotite xenoliths at present available for study.

Lesser Antilles

The island of Grenada in the Lesser Antilles island arc provides us with a range of mafic to ultramafic xenoliths (e.g. Arculus & Wills, 1980; Parkinson *et al.*, 2003) derived from the lower crust and lithospheric mantle. Alkali olivine basalts host the xenoliths. The peridotite xenoliths are anhydrous, and modally divided into dunites, harzburgites and lherzolites, although the lherzolites appear to be metasomatic products from original harzburgites (Fig. 3j; Parkinson *et al.*, 2003). The metasomatic addition of clinopyroxene at the expense of orthopyroxene appear to be a characteristic of the Grenada peridotite xenolith suite (Parkinson *et al.*, 2003).

Some of the Grenada peridotites plot off the olivine–spinel mantle array (Fig. 4k), consistent with their genesis as a metasomatic product (Parkinson *et al.*, 2003). The Cr-number of spinel is higher than 0·3 (Figs 4k, 5k and 6k) indicating an initial refractory protolith mineralogy as suggested by Parkinson *et al.* (2003). The high Cr-number of spinel resulted from equilibration with an oxidized melt during the metasomatism (Parkinson *et al.*, 2003). The Mg-number–Cr-number relationship of spinel is the same for all the peridotites irrespective of the Fo content of the coexisting olivine (Fig. 5k), possibly as a result of the high temperatures (around 1200°C) of the metasomatism (Parkinson *et al.*, 2003). Chromian spinels are characterized by relatively high γ_{Fe} values (around 0·1) (Fig. 6k). Clinopyroxenes are very low in Na irrespective their origin, primary or metasomatic (Parkinson *et al.*, 2003) (Fig. 7k). The calculated equilibration temperatures are highly variable from *c.* 800 to 1200°C (Fig. 9k). This may be due to multiple equilibrium stages, including subsolidus equilibration after partial melting and high-temperature re-equilibration during the metasomatism (Parkinson *et al.*, 2003). The Grenada peridotites have notably high oxygen fugacity (Fig. 10k), consistent with the relatively high γ_{Fe} of the chromian spinel (Fig. 6k).

Pannonian Basin

The Carpathian–Pannonian Basin (subsequently referred to as the Pannonian Basin here) in central Europe experienced subduction-related megmatism in late Cretaceous to Tertiary times, although the plate tectonic reconstructions are somewhat contentious (e.g. Csontos, 1995; Csontos & Vörös, 2004). Calc-alkaline volcanism is recognized in the northern part of the Carpathian–Pannonian region (e.g. Szabó *et al.*, 1992), and thus peridotite xenoliths exhumed by subsequent alkali basaltic volcanism of Pliocene–Pleistocene in the same region (e.g. Szabó *et al.*, 1992) might be expected to record some mantle-wedge processes associated with the earlier subduction.

Lherzolites are predominant over harzburgites in the Pannonian Basin xenolith suites (Fig. 3k; e.g. Embey-Isztin *et al.*, 2001; Szabó *et al.*, 2004). The peridotites mostly plot within the olivine–spinel mantle array (Fig. 4l). The Cr-number of chromian spinels exhibits a wide range, from 0·1 to 0·6, but is mostly lower than 0·3 (Figs 4l and 5l), consistent with the clinopyroxene-rich modal compositions (Fig. 3k). The γ_{Fe} of spinel is generally low, <0·1 (Fig. 6l). The Pannonian Basin peridotites are similar in the chemistry of their olivine and spinel to abyssal peridotites (Figs 4l, 5l and 6l). The Na_2O content of the clinopyroxenes is, however, higher than in abyssal peridotites at a given Cr-number of spinel (Fig. 7l). The Na_2O content of clinopyroxene vs Cr-number of spinel relationship (Fig. 7l) is broadly similar to that of the peridotite xenoliths from SW Japan (Fig. 7c). It is possible that the Pannonian Basin peridotites have a hybrid character between abyssal peridotites and continental rift-zone peridotites (Fig. 7l). Hydrous minerals have slightly higher Ti contents than those in the West Pacific arc xenoliths (Fig. 8i), but are similar to equivalents from the Megata volcano of the NE Japan arc (Fig. 8b). Sulfides in the Pannonian Basin peridotites show a wide range of Fe/Ni ratios (e.g. Szabó *et al.*, 2004), partly as a result of their origin by low-temperature decomposition from primary MSS (monosulfide solid solutions) globules. The equilibrium temperature is dependent on texture, being higher in coarse-grained protogranular xenoliths than in fine-grained equigranular ones (Szabó *et al.*, 2004). According to our calculations, most of the xenoliths exhibit equilibrium tempratures of 900–1000°C (Fig. 9l). The Pannonian Basin peridotites are similar in redox state to abyssal peridotites (Fig. 10l).

The mantle peridotite xenoliths from the Pannonian Basin generally lack features suggesting a strong influence from a subducting slab; for example, a high degree of partial melting induced by slab-derived aqueous fluids, silica enrichment and the metasomatic formation of Ti-poor hydrous minerals (see Dobosi *et al.*, 1999). However, the presence of glass inclusions or pockets

and carbonate–silicate glass veinlets in some xenoliths may be indicative of involvement of some slab-derived materials (e.g. Szabó *et al.*, 1996; Demény *et al.*, 2004).

PETROLOGICAL SKETCH OF THE FORE-ARC MANTLE PERIDOTITE

Peridotites exhumed from the fore-arc ocean floor are assumed to be representative of the very corner of the mantle wedge, and are briefly described here although they are not of xenolithic origin (Fig. 1l). They have been dredged or drilled from serpentinite seamounts or the arc-ward wall of the trench in oceanic arcs since the pioneering work of Fisher & Engel (1969) and Bloomer (1983). The arcs of Tonga (e.g. Bloomer & Fisher, 1987), Izu–Bonin–Mariana (e.g. Bloomer & Hawkins, 1983; Ishii, 1985; Parkinson & Pearce, 1998; Okamura *et al.*, 2006) and South Sandwich (e.g. Pearce *et al.*, 2000) provide us with good examples. Peridotitic rocks from the Mariana arc are the most extensively studied (see Fryer, 1996).

The fore-arc peridotites are typically more depleted than abyssal peridotites, except for some lherzolites from the South Sandwich arc (Pearce *et al.*, 2000) (Fig. 1la–d; see Arai, 1994). The South Sandwich lherzolites are plagioclase-bearing and were derived from a trench–fracture zone intersection area (Pearce *et al.*, 2000). The fore-arc peridotites are mostly harzburgites with high-Cr-number (>0·4) chromian spinel (Fig. 1lb–d). The Mg-number of spinel is lower in the fore-arc peridotites than in abyssal peridotites at a given Cr-number (Fig. 1lc; Ishii *et al.*, 1992) as a result of the lower equilibrium temperatures of the former (Okamura *et al.*, 2006). As expected, the Na_2O content of the clinopyroxene is low in the fore-arc peridotites (Fig. 1le). Hydrous minerals (amphiboles and phlogopite) are characterized by low Ti contents relative to alkalis (Fig. 1lf).

It is noteworthy that the fore-arc peridotites (lherzolite to harzburgite) from the South Sandwich arc are very similar to some abyssal peridotite (Fig. 1l), except for dunites with high-Cr-number (0·7–0·8) spinel (Pearce *et al.*, 2000). The dunite that contains chromian spinel with high Cr-number and low Ti (<0·3 wt % of TiO_2) is associated with arc magmatism (see Arai, 1992). This combination, abyssal peridotite + arc-type dunite, is reminiscent of the mantle section of some ophiolites (e.g. Andal *et al.*, 2005; Arai *et al.*, 2006*a*).

DISCUSSION

Partial melting

The degree of depletion appears to be highly variable in the range of mantle-wedge peridotites considered here. This can be as high as in abyssal peridotites in terms of modal and mineral chemical compositions (Figs 3–6). Some of the mantle-wedge peridotites (e.g. those from the Canadian Cordillera, central Mexico and the Carpathian–Pannonian Basin) are more fertile than the most fertile abyssal lherzolites (Figs 3–6). In contrast, other mantle-wedge peridotites (e.g. those from the Avacha and Iraya volcanoes) are distinctly more depleted than the most depleted abyssal peridotite (Figs 3–6). This lithological variation is probably due to the complex tectonic history of each arc (e.g. Karig, 1971; Uyeda & Kanamori, 1979) as well as to across-arc variation in magma production conditions (e.g. Sugimura *et al.*, 1963; Kuno, 1966; Tatsumi *et al.*, 1983; Tatsumi, 1986). The lithospheric mantle below those arcs located on oceanic lithosphere, such as the Aleutian arc, is basically composed of abyssal peridotite, which has been subsequently modified by arc magmatism or metasomatism by slab-derived agents to various extents (see Kay & Kay, 1986). Other arcs developed on continental lithosphere, such as the Andean arc or the SW Japan arc, overlie subcontinental lithospheric mantle, which might have had a long history of previous depletion and enrichment events before being modified by arc magmatism and metasomatism (see Arai *et al.*, 2007).

The common occurrence of harzburgite xenoliths within arc-front volcanoes (e.g. Avacha volcano, Kamchatka and Iraya volcano, Luzon–Taiwan arc) may indicate high-degree partial melting or depletion around the corner of the mantle wedge. The harzburgites plot outside the abyssal peridotite field in panels a, d and e of Figs 3–6. This is consistent with higher magma production rates at the volcanic front than in the rear-arc region of arcs (Sugimura *et al.*, 1963), possibly because the supply of slab components (mainly aqueous fluids) is stronger beneath the volcanic front (see Tatsumi, 1986). It is noteworthy that some of the harzburgite xenoliths with high-Cr-number spinel exhibit relatively low-Fo olivine (Fig. 4); also the Cr-number of spinel is variable at a constant Fo content of the coexisting olivine. A good example is available from the Avacha volcano (Fig. 4a), for which Ishimaru *et al.* (2007) interpreted the harzburgite as a residue after partial melting assisted by relatively low-Mg-number fluid flux. The discrete pargasite in the Avacha harzburgite (Fig. 2a) was interpreted as a primary residual phase formed during hydrous partial melting (Ishimaru *et al.*, 2007).

Depleted harzburgite xenoliths have been recorded from rear-arc or back-arc regions of some arcs. The Oshima-Ôshima volcano within the Sea of Japan (a back-arc basin) off Hokkaido, the most continent-ward volcano of the NE Japan arc (Figs 4b, 5b and 6b; Ninomiya & Arai, 1992) is a good example. The Oshima-Ôshima volcano lies on the edge of the Japan Sea basin close to the

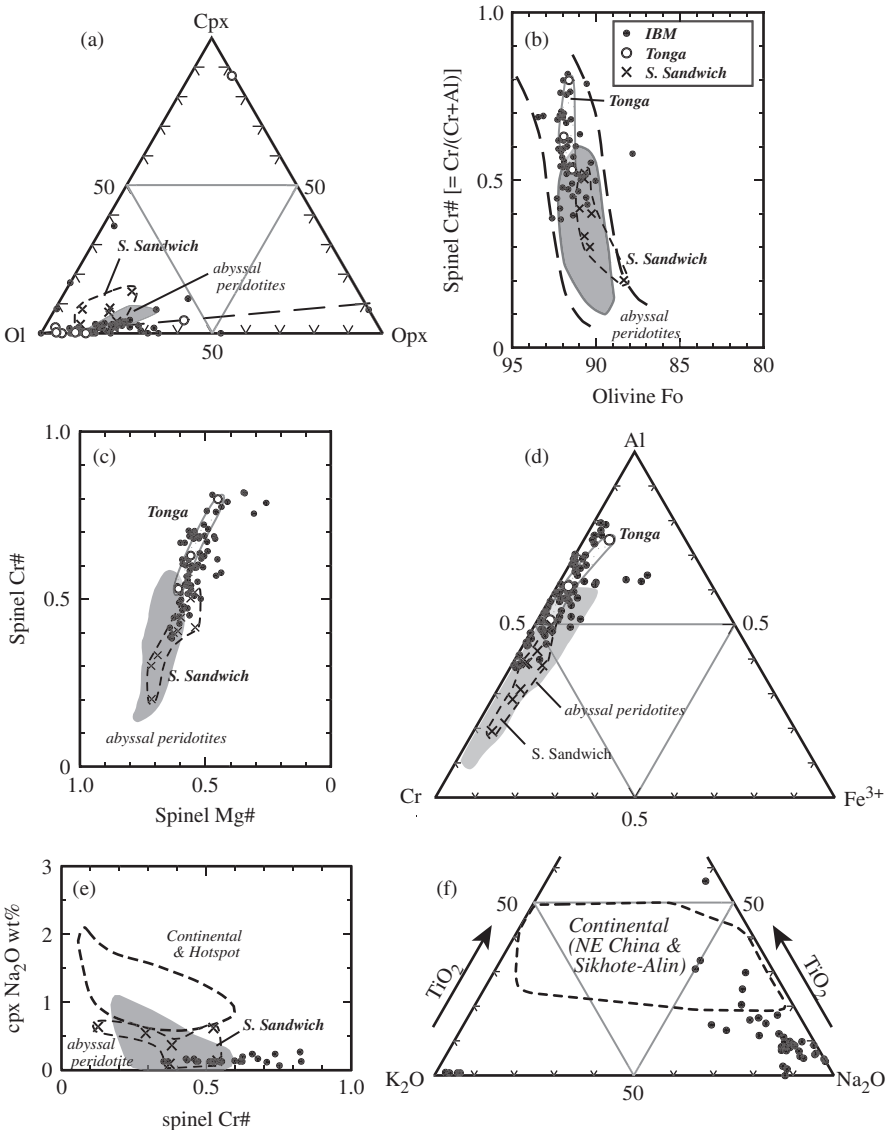

Fig. 11. Petrological and mineral chemical characteristics of fore-arc peridotites. Samples were dredged or drilled from the ocean floor of the Izu–Bonin–Mariana (IBM), Tonga and South Sandwich arcs. (a) Modal compositions. (b) Cr-number of olivine vs Fo content of olivine. (c) Cr-number vs Mg-number of chromian spinel. (d) Trivalent cation ratios of chromian spinel. (e) Na_2O of clinopyroxene vs Cr-number of chromian spinel. (f) TiO_2–K_2O–Na_2O weight ratios of hydrous minerals (amphiboles and phlogopite). Symbols as in (b). Data sources: Bloomer & Hawkins (1983), Ishii (1985), Ishii *et al.* (1992, 2000), Ohara & Ishii (1998), Parkinson & Pearce (1998) and Okamura *et al.* (2006) for IBM; Bloomer & Fisher (1987) for the Tonga arc: Pearce *et al.* (2000) for the South Sandwich arc. (See Figs 2–7 for further explanation.)

continental-type lithosphere of the NE Japan arc. Harzburgite is also common in the xenolith suite from the Megata volcano, one of the rear-arc volcanoes of the NE Japan arc (Figs 3b, 4b, 5b and 6b). This is consistent with the occurrence of the Takeshima harzburgites from the Sea of Japan, which are interpreted as residues of back-arc basin basalt formation (Ninomiya *et al.*, 2007). The high-temperature peridotites, including the harzburgite from Noyamadake in the SW Japan arc (Hirai, 1986) and from Alligator Lake and others within the northern Canadian Cordillera (e.g. Shi *et al.*, 1998), are possibly derived from high-temperature asthenosphere upwelling through a slab window during back-arc extension, with or without back-arc basin opening. Partial melting may have been assisted by fluid flux from the subducted slab (Abe & Arai, 2005). The frequent occurrence of depleted harzburgites in the rear-arc or back-arc regions of arcs is probably a consequence of the upwelling of asthenospheric mantle, assisted by slab-derived fluid flux to some extent.

Refractory dunites possibly formed by harzburgite–melt reaction (Quick, 1981; Kelemen, 1990) have been found from the lithospheric mantle beneath arcs (e.g. Arai & Abe, 1994; Bryant *et al.*, 2007). Such dunites are expected to be common beneath some parts of arcs where magmas actively pass through lithospheric mantle peridotite.

Metasomatism

Studies of xenoliths exhumed from the supra-subduction zone mantle wedge have highlighted metasomatism-related features that may be distinctive to this tectonic setting. We discuss here the silica-enrichment process, formation of hydrous minerals (hydration) and precipitation of sulfide minerals within the mantle wedge.

Silica enrichment

Some of the depleted harzburgite xenoliths derived from the mantle wedge beneath the volcanic front exhibit metasomatic silica enrichment; that is, the formation of secondary orthopyroxene at the expense of olivine induced by slab-derived fluids or melts (Fig. 2b–e). This process was predicted by Kesson & Ringwood (1989) although its effectiveness in enriching the mantle in silica has been debated (e.g. Canil, 1992; Kelemen *et al.*, 1998).

The metasomatic secondary orthopyroxene in the peridotite xenoliths from the Avacha, Shiveluch and Iraya volcanoes is characterized by low contents of CaO, Al_2O_3 and Cr_2O_3 relative to the primary orthopyroxene (e.g. Arai *et al.*, 2003; Figs 12a and 13a). The Mg-number is, however, almost the same (>0·9) in the primary and secondary orthopyroxenes (Arai *et al.*, 2003, 2004; Ishimaru *et al.*, 2007). The secondary orthopyroxene from the TUBAF seamount, Papua New Guinea (e.g. McInnes *et al.*, 2001; Franz *et al.*, 2002), displays almost the same petrographic and chemical characteristics as that in other Western Pacific peridotite xenoliths (Figs 12a and 13a). The secondary orthopyroxene in the Avacha and Iraya xenoliths was formed via reaction between olivine and slab-derived aqueous fluids containing a dissolved silicate component, which were supplied via arc magmas or directly from the slab (e.g. Arai *et al.*, 2003, 2004; Ishimaru *et al.*, 2007). Small amounts of secondary hydrous minerals (tremolite to pargasite and phlogopite) are associated with the secondary orthopyroxene in some of Avacha harzburgite xenoliths (Ishimaru *et al.*, 2007), especially in the fine-grained peridotites (Ishimaru & Arai, 2008). This is consistent with the involvement of an aqueous fluid. The aqueous fluids in equilibrium with mantle peridotite, irrespective of the ultimate origin of the fluids, are rich in SiO_2 relative to MgO (e.g. Nakamura & Kushiro, 1974; Mibe *et al.*, 2002), and have the potential to convert olivine to orthopyroxene on metasomatism.

Orthopyroxene with very low Ca and Al contents was first reported from peridotite xenoliths from the Colorado Plateau by Smith and coworkers (Riter & Smith, 1996; Smith & Riter, 1997; Smith *et al.*, 1999). Textural relationships indicating replacement of olivine by this orthopyroxene are, however, not so distinct compared with the secondary orthopyroxene from the Western Pacific xenoliths, possibly because of the older age of formation (see Smith, 2000). Some of the orthopyroxenes in xenoliths from the Colorado Plateau (Riter & Smith, 1996; Smith & Riter, 1997; Smith *et al.*, 1999) and Simcoe (Ertan & Leeman, 1996) plot in the field of the secondary orthopyroxene with a distinct replacement texture (Fig. 2b and e) from the Western Pacific (Figs 12c and 13c), although they are not distinct texturally from the primary orthopyroxenes. This suggests that the orthopyroxene low in CaO, Al_2O_3 and Cr_2O_3 from the Colorado Plateau xenoliths could be of the same origin as that in the Western Pacific harzburgite xenoliths, as originally suggested by Riter & Smith (1996), Smith & Riter (1997) and Smith *et al.* (1999).

The orthopyroxenes in the depleted peridotite xenoliths from the Lesser Antilles (Parkinson *et al.*, 2003) are generally very low in Ca (Fig. 12f), although the nominal equilibration temperatures are not particularly low (Fig. 9k). Their CaO content (<0·2 wt %; Parkinson *et al.*, 2003) is lower than that of the primary orthopyroxene (Fig. 12k) in the more depleted Avacha peridotites (Fig. 4a and k). This may indicate disequilibrium or imperfect equilibrium between the two pyroxenes in the Lesser Antilles peridotites. Some of the Lesser Antilles orthopyroxenes are also low in Al_2O_3 and Cr_2O_3 (Figs 12f and 13f). We suggest that at least some of the orthopyroxenes from the Lesser Antilles peridotites were initially formed in the same manner as the secondary orthopyroxene from the Western Pacific harzburgite xenoliths. They have subsequently been texturally modified through recrystallization, but have retained to some degree their initial chemical characteristics of low contents of CaO, Al_2O_3 and Cr_2O_3. The Lesser Antilles peridotites were initially dunites to harzburgites, and the metasomatic addition of orthopyroxene and subsequently clinopyroxene and olivine at the expense of orthopyroxene (Parkinson *et al.*, 2003) has determined their current mineralogy. The apparently primary orthopyroxenes from peridotite xenoliths other than those of the Lesser Antilles are high in CaO, Al_2O_3 and Cr_2O_3, and are distinguishable from the secondary orthopyroxenes in the Western Pacific peridotite xenoliths (Figs 12 and 13).

Plume–mantle wedge interaction

Plume or hot asthenospheric mantle intruded into the mantle wedge through a slab window could cause decompression-induced partial melting, which could metasomatically modify the pre-existing peridotite, as in the case of the SW Japan arc. Here plume-related alkali basalts precipitated pyroxenites composed of black pyroxenes,

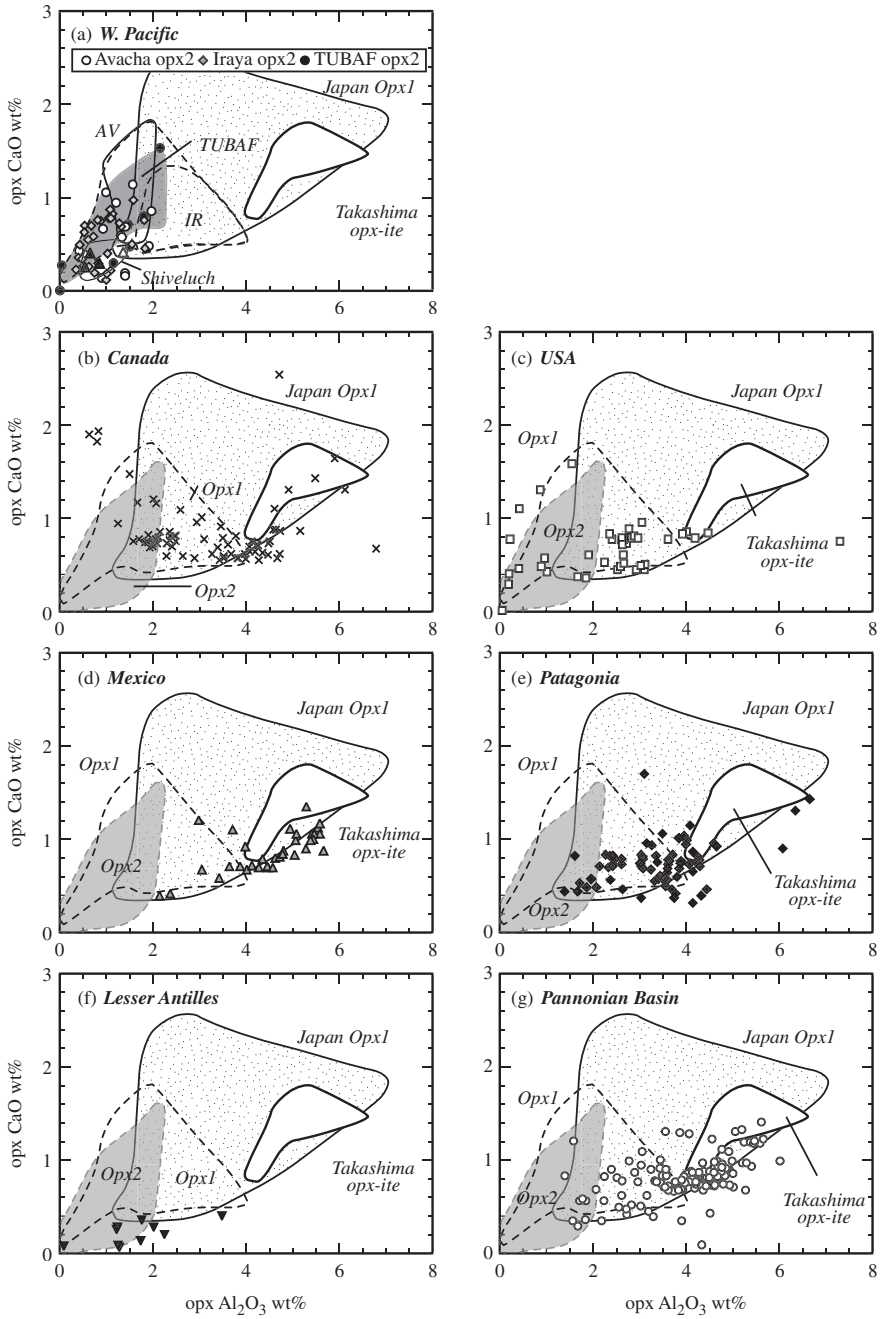

Fig. 12. Relationship between CaO and Al_2O_3 contents in the secondary olivine-replacing orthopyroxene in peridotite xenoliths from the mantle wedge as compared with other mantle orthopyroxenes. Fields for primary orthopyroxenes (Opxl) in peridotite xenoliths from the Japan arcs (Takahashi, 1978*b*; Hirai, 1986; Goto & Arai, 1987; Abe *et al.*, 1992, 1995, 2003; Ninomiya & Arai, 1992; Abe, 1997) and the secondary orthopyroxenes precipitated from an evolved alkaline magma from Takashima (Arai *et al.*, 2006*b*) are shown for comparison. Fields for the primary and secondary orthopyroxenes from Avacha (AV), Iraya (IR) and TUBAF are shown in (b)–(h) for comparison. (See text for detailed discussion.) (a) Western Pacific arcs (including TUBAF). Secondary orthopyroxenes (Opx2) from three arcs are plotted in comparison with primary orthopyroxenes (fields for AV, IR and TUBAF) for each. It should be noted that the secondary orthopyroxenes are lower in Ca and Al than the primary ones. Data from Arai *et al.* (2003) and Ishimaru *et al.* (2007) for Avacha, from Bryant *et al.* (2007) for Shiveluch, from Arai & Kida (2000) and Arai *et al.* (2004) for Iraya, and from Franz & Wirth (2000), McInnes *et al.* (2001), and Franz *et al.* (2002) for TUBAF. (b) Canadian Cordillera. Data from Francis (1987), Shi *et al.* (1998), Peslier *et al.* (2002), and Harder & Russell (2006). (c) Western USA. Data from Draper (1992), Brandon & Draper (1996), Ertan & Leeman (1996), Riter & Smith (1996), Smith & Riter (1997), Ducea & Saleeby (1998), Smith *et al.* (1999) and Downes *et al.* (2004). (d) Central Mexico. Data from Heinrich & Besch (1992), Luhr & Aranda-Gómez (1997) and Blatter & Carmichael (1998). (e) Patagonia. Data from Gorring & Kay (2000), Laurora *et al.* (2001), Kilian & Stern (2002), Rivalenti *et al.* (2004*a*, 2004*b*), Bjerg *et al.* (2005) and Shilling *et al.* (2005). (f) Lesser Antilles. Data from Parkinson *et al.* (2003). (g) Pannonian Basin. Data from Szabó & Taylor (1994), Downes *et al.* (1995), Konečný *et al.* (1995), Szabó *et al.* (1995), Vaselli *et al.* (1995), Dobosi *et al.* (1999) and Embey-Isztin *et al.* (2001).

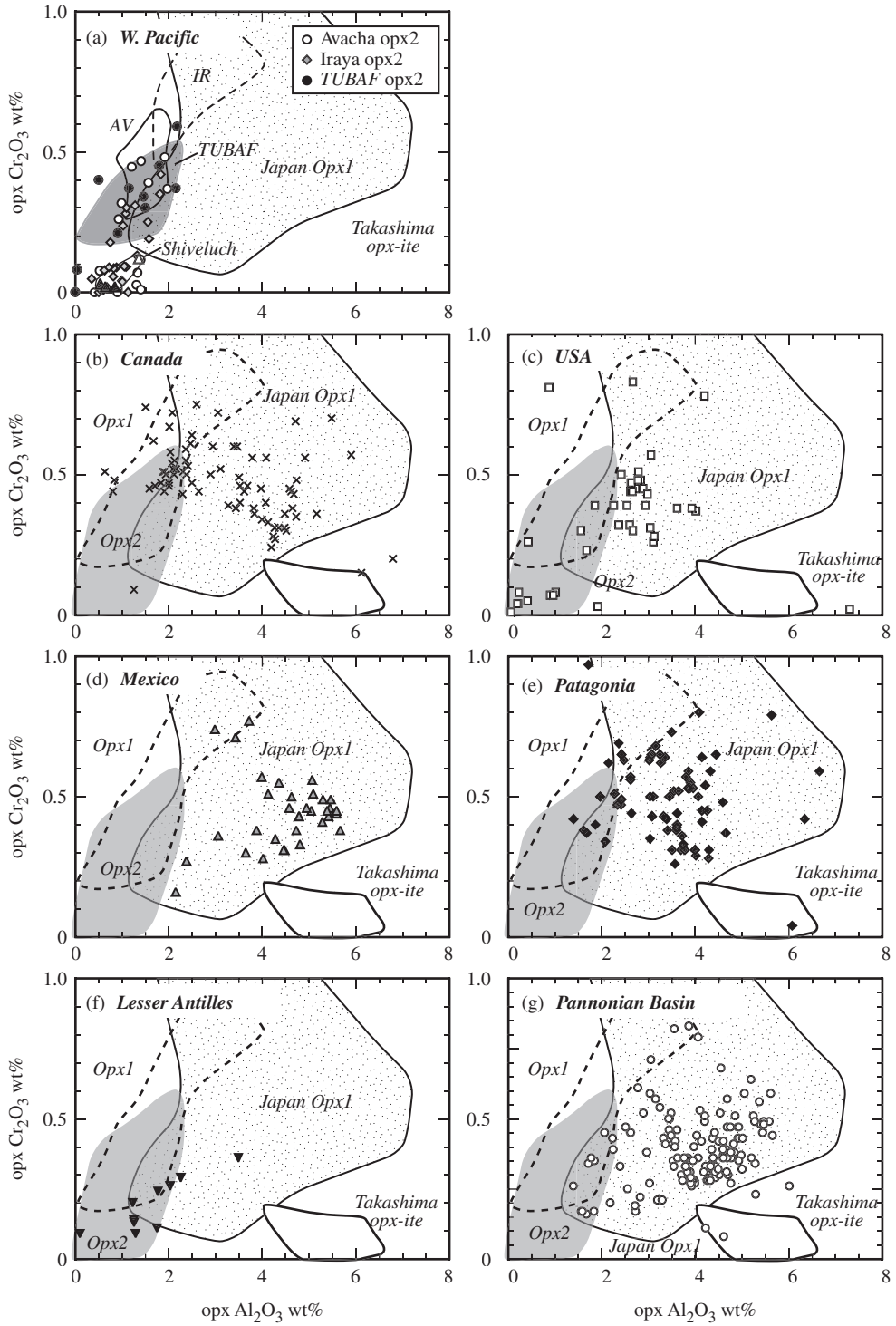

Fig. 13. Relationship between Cr_2O_3 and Al_2O_3 contents in the secondary olivine-replacing orthopyroxene in peridotite xenoliths from the mantle wedge as compared with other mantle orthopyroxenes. Sources of data are the same as in Fig. 12.

which were entrained as Group II (Frey & Prinz, 1978) xenoliths by younger alkali basalts from the same asthenospheric upwelling (e.g. Arai *et al.*, 2000). The silicate melt involved in the precipitation of the Group II pyroxenites in the mantle affected the peridotite chemistry (Arai *et al.*, 2000). The iron-rich peridotites from Shingu (Goto & Arai, 1987) and Oki-Dogo (Abe *et al.*, 2003) plot off the olivine–spinel mantle array, in Fig. 4c, and may represent such

an alkali basaltic metasomatized mantle wedge (see Arai *et al.*, 2000).

Recently, Arai *et al.* (2006*b*) reported a new type of orthopyroxenite replacing mantle olivine in tectonized dunite and wehrlite xenoliths form Takashima in the SW Japan arc. This orthopyroxenite also occurs as discrete xenoliths in addition to thin veinlets in peridotites. In both cases, it clearly shows a texture indicating replacement of olivine (Arai *et al.*, 2006*b*). Other silicates (plagioclase and clinopyroxene) are sometimes found at the interior of the veins. The secondary orthopyroxene from Takashima is, however, remarkably different in chemistry from other secondary orthopyroxenes; its Mg-number is highly variable depending on the thickness of the orthopyroxenite veinlets, from >0·9 in thin veinlets to 0·7 in thick veins or discrete xenoliths (Arai *et al.*, 2001, 2006*b*). It has higher CaO, Al_2O_3 and Cr_2O_3 contents than the other secondary orthopyroxenes (Figs 12a and 13a). The melt involved in precipitation of this type of orthopyroxene is not a slab-derived silicic melt but a melt evolved from an alkali basalt with moderate silica undersaturation (Arai *et al.*, 2006*b*). All of the secondary orthopyroxenes formed from slab-derived fluids or melts are distinct from those produced by infiltration of alkali basaltic melts within the upper mantle (Figs 12a and 13a).

The back-arc region of the southernmost part of the Andean arc (Patagonia) is distinguished by carbonatite metasomatism in the upper mantle (e.g. Gorring & Kay, 2000; Laurora *et al.*, 2001; Rivalenti *et al.*, 2004*b*). This is possibly a manifestation of one of the mantle processes associated with slab-window magmatism (e.g. Gorring & Kay, 2001). Carbonatite metasomatism within the mantle wedge (above a subducted slab) has not been clearly recognized, although the possibility of such metasomatic agents has been discussed (Ikehata & Arai, 2004).

Hydration

As described above, the formation of secondary hydrous minerals that are not apparently associated with the olivine-replacing secondary orthopyroxene is common in mantle-wedge peridotite xenoliths. The pargasite and phlogopite within the peridotite xenoliths from the Western Pacific arcs are low in TiO_2 relative to those in peridotite xenoliths from the eastern margin of the Eurasian continent (Fig. 8a–c; Arai *et al.*, 2007). Aoki & Shiba (1973) suggested that the metasomatic agent was essentially an aqueous fluid based on major- to minor-element budgets on hydration. This interpretation is consistent with the relative deficiency in Ti, one of the HFSE, in the slab-derived fluid or a fluid released from rising arc magmas (e.g. Keppler, 1996). The low Ti content of the amphiboles in hydrated peridotites from the Colorado Plateau (Smith, 1979; Smith *et al.*, 1999) and of phlogopites in the Bearpaw Mountains peridotites from the Wyoming craton (Downes *et al.*, 2004) (Fig. 8f) is consistent with involvement of aqueous fluids associated with subduction, as suggested by Smith *et al.* (1999) and Downes *et al.* (2004).

In contrast, the metasomatic hydrous minerals in continental peridotite xenoliths are relatively high in TiO_2 (e.g. Arai *et al.*, 2007). This is consistent with their generation by reaction with infiltrating alkaline intra-plate magmas, which are relatively high in HFSE (e.g. Pearce & Cann, 1973). In this context, the high TiO_2 content of phlogopite in the peridotite xenoliths from Kostal Lake in the Canadian Cordillera (Canil & Scarfe, 1989) might be related not to slab-derived fluids but to an intra-plate basaltic magma released from asthenosphere upwelling through a slab window. Hydrous minerals in the central Mexican peridotite xenoliths (Luhr & Aranda-Gómez, 1997; Blatter & Carmichael, 1998) are relatively high in TiO_2 (Fig. 8g). The high-Ti phlogopite from Ventura–Espíritu Santo at the farthest distance from the paleotrench (Luhr & Aranda-Gómez, 1997) may have been formed in the same setting as the Kostal Lake phlogopite (Canil & Scarfe, 1989); that is, back-arc extension driven by asthenospheric injection (see Shi *et al.*, 1998). Hornblende in the El Peñon peridotites (Blatter & Carmichael, 1998) is slightly higher in Ti than the low-Ti pargasites from other mantle wedge peridotites (Avacha, Shiveluch, Iyara, Megata and TUBAF volcanoes; Fig. 8a–d), possibly because of the more evolved character of the infiltrating melt in the former.

Redox state of the mantle wedge

It is well known that some mantle-wedge peridotites are characterized by relatively high oxygen fugacities (e.g. Brandon & Draper, 1996; Parkinson & Arculus, 1999). The summary in Fig. 10 indicates that some peridotite xenoliths from the Western Pacific (Avacha, Shiveluch, Iraya, Megata and TUBAF) have average oxygen fugacities higher than those of abyssal peridotite. Most of them are also highly metasomatized, as described above. In the Avacha xenolith suite, the fine-grained highly metasomatized peridotites have a higher oxygen fugacity on average than the less metasomatized coarse-grained peridotites (e.g. Arai *et al.*, 2003). This indicates that metasomatism involving the precipitation of hydrous phases might be linked with the high oxidation state (e.g. Brandon & Draper, 1996; Parkinson & Arculus, 1999). The Lesser Antilles peridotite xenoliths also indicate highly oxidized equilibrium conditions (Fig. 10k), possibly consistent with the metasomatic formation of some of the orthopyroxene as discussed above.

The process by which mantle oxygen fugacity is increased is, however, little understood. Peridotites with little apparent metasomatism have high oxygen fugacity values in some xenolith suites (Parkinson & Arculus, 1999; Bryant *et al.*, 2007). High sulfur fugacity may stabilize sulfides by reaction between mantle olivine and

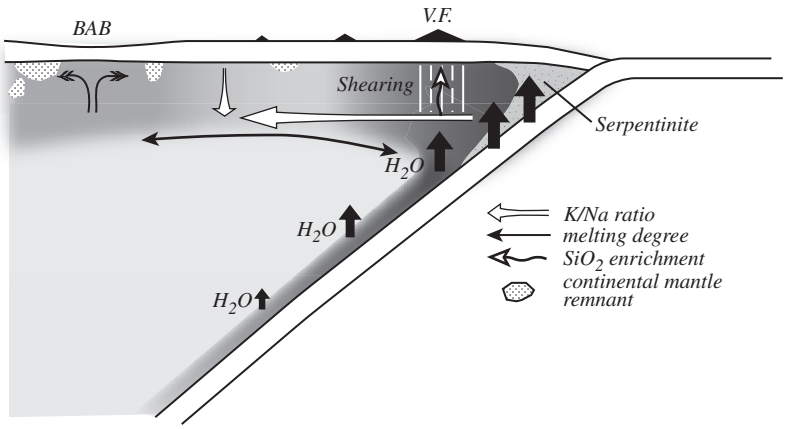

Fig. 14. Sketch of the lithosphere part of the mantle wedge based on observations on xenoliths: an example of a volcanic arc that has developed on a continental margin. The degree of depletion of peridotite increases towards both the corner of the wedge and the back-arc region. Enrichment in silica is prominent beneath the volcanic front. K/Na ratio of metasomatized peridotite may increase both downward and towards the corner within the lithosphere. (See text for discussion.)

sulfur-bearing fluids, which can release oxygen to oxidize the metasomatized peridotites. Further studies are required to resolve this issue.

Shearing within the mantle wedge

The extremely fine-grained peridotite xenoliths [F-type peridotites of Arai *et al.* (2003)] (Fig. 2c) are characteristically found within volcanoes on the volcanic front; for example, the Avacha and Shiveluch volcanoes of the Kamchatka arc (e.g. Arai *et al.*, 2003; Bryant *et al.*, 2007) and the Iraya volcano of the Luzon–Taiwan arc (e.g, Arai *et al.*, 1996, 2004). Arai *et al.* (2004) suggested that their grain size might be linked to shearing. The shearing is a consequence of transcurrent movement of the overlying mantle wedge during oblique subduction of a slab as suggested by Fitch (1972). The occurrence of this type of xenolith exclusively within volcanic-front volcanoes could be consistent with the prediction of Fitch (1972) that strike-slip faults form around the volcanic front. The fine-grained peridotites from Avacha and Iraya were possibly derived from deep extensions of such strike-slip faults into the lithospheric mantle beneath the eastern margin of the Eurasian continent. A sinistral NE–SW-trending strike-slip fault system has been prominent since Permian times in East Asia (e.g. Xu *et al.*, 1989; Lee, 1999).

Petrological model of the lithospheric mantle beneath arcs

A simplified petrological model for the lithospheric part of the mantle wedge is shown in Fig. 14. Peridotites are highly hydrated around the corner of the wedge (Fig. 14; Tatusmi, 1986). The asthenospheric part of the wedge cannot be directly understood through xenolith studies.

The degree of depletion of the mantle peridotite before metasomatism appears to decrease from the fore-arc to the back-arc region of the mantle wedge. The highly refractory harzburgite frequently found within the fore-arc region to the volcanic front represents residual mantle after past (fore-arc) or present (volcanic front) magma production. The degree of depletion of the peridotite may increase again towards back-arc basins that have a fast opening rate such as the Sea of Japan. The across-arc petrological heterogeneity of the lithospheric mantle depends on the presence or absence of back-arc spreading, and also on the spreading rate.

The degree of metasomatic modification of the mantle wedge (hydration, silica enrichment and sulfide formation) decreases from the volcanic front towards the back-arc region because the supply of aqueous fluids from the progressively dehydrating slab probably decreases with increasing depth to the subducting slab (e.g. Tatsumi, 1986). The strong metasomatism observed in peridotite xenoliths from volcanoes on the volcanic front is a consequence of this process.

Shearing associated with metasomatism is prominent in the lithospheric mantle at the volcanic front (Arai *et al.*, 2004; Fig. 14). This is due to transcurrent movement in the corner of the mantle wedge caused by oblique subduction (Fitch, 1972). This sheared part of the mantle wedge possibly serves as a pathway for fluids or melts migrating from the asthenosphere. This phenomenon is observable only through xenoliths from the arc-front volcanoes.

The K/Na ratio in the metasomatized peridotites is also highly variable (see Brandon *et al.*, 1999). Potassium is fractionated from sodium during upward movement of

the metasomatizing fluid (Arai, 1986) because the stability fields of K-rich minerals (phlogopite and potassic richterite) (e.g. Kushiro *et al.*, 1967; Forbes & Flower, 1974; Gilbert *et al.*, 1982; Konzett & Ulmer, 1999) extend to higher pressures than those of Na-rich minerals (hornblende) (e.g. Gilbert, 1969; Holloway, 1973; Niida & Green, 1999). Potassium is preferentially incorporated into the mantle at higher pressures (phologopite stability field), and residual high Na/K fluids (or melts) precipitate hornblende at shallower depths.

Sodium is preferentially removed from the slab at shallower depths than potassium (see Brandon *et al.*, 1999), which may give rise to an increase in the K/Na ratio of the metasomatized mantle towards the back-arc region. This is consistent with the predominance of metasomatic amphibole over phlogopite in the fore-arc mantle peridotites (e.g. Ohara & Ishii, 1998; Okamura *et al.*, 2006). The predominance of phlogopite in the Bearpaw Mountains peridotites, which is interpreted to have been formed by slab-derived fluids probably at a considerable distance from a trench (Downes *et al.*, 2004), is also consistent with the interpretation above.

The mantle wedge may contain exotic fragments that are remnants of previous geodynamic settings. Their origin depends on the tectonic setting of the arc. The upper mantle below the Aleutian arc, which is constructed on oceanic lithosphere, may contain fragments of abyssal mantle (see Kay & Kay, 1986). In the case of some Western Pacific arcs that have developed on the Eurasian continental margin, the lithospheric mantle beneath the arcs to back-arc basins possibly contains fragments of sub-continental lithospheric mantle (Fig. 14; Ninomiya *et al.*, 2007).

ACKNOWLEDGEMENTS

We acknowledge many persons including N. Abe, H. Hirai, Y. Shimizu, K. Goto, A. Ninomiya, Y. Kobayashi, Y. Saeki, M. Fujiwara, and H. Shukuno for their collaboration in sampling and analysis of xenoliths. We are especially grateful to N. Abe and H. Hirai for their discussion about the sub-arc mantle xenoliths. We thank A. Ishiwatari, T. Morishita and Y. Ishida for their discussion and support in mineral chemical analysis. We appreciate critical comments of L. Franz and two anonymous referees, which were helpful in revising the previous manuscript. We also appreciate M. Wilson, the Editor, for her detailed comments and editorial handling. This work is partially supported by Grant-in-Aid for Creative Scientific Research (19GS0211).

REFERENCES

Abe, N. (1997). Petrology of mantle xenoliths from the arcs: Implications for the petrochemical evolution of the wedge mantle. PhD thesis, Kanazawa University.

Abe, N. & Arai, S. (2001). Comments on 'Garnet-bearing spinel harzburgite xenolith from Arato-yama alkali basalt, southwest Japan' by Yamamoto et al. *Journal of Mineralogical and Petrological Sciences* **30**, 190–193 (in Japanese with English abstract).

Abe, N. & Arai, S. (2005). Petrography and geochemistry of the mantle xenoliths: Implications for lithospheric mantle beneath the Japan arcs. *Japanese Magazine of Mineralogical and Petrological Sciences* **34**, 143–158 (in Japanese with English abstract).

Abe, N., Arai, S. & Saeki, Y. (1992). Hydration processes in the arc mantle; petrology of the Megata peridotite xenoliths, the Northeast Japan arc. *Journal of Mineralogy, Petrology and Economic Geology* **87**, 305–317 (in Japanese with English abstract).

Abe, N., Arai, S. & Ninomiya, A. (1995). Peridotite xenoliths and essential ejecta from the Ninomegata crater, the Northeastern Japan arc. *Journal of Mineralogy, Petrology and Economic Geology* **90**, 41–49 (in Japanese with English abstract).

Abe, N., Arai, S. & Yurimoto, H. (1998). Geochemical characteristics of the uppermost mantle beneath the Japan island arcs: implications for upper mantle evolution. *Physics of the Earth and Planetary Interiors* **107**, 233–247.

Abe, N., Arai, S. & Yurimoto, H. (1999). Texture-dependent geochemical variations of sub arc mantle peridotite from Japan island arcs. In: Gurney, J. J., Gurney, J. L., Pascoe, M. D. & Richardson, S.H. (eds) *Proceedings of VIIth International Kimberlite Conference, J.B. Dawson Volume*. Cape Town: Red Roof Design, pp. 13–22.

Abe, N., Takami, M. & Arai, S. (2003). Petrological feature of spinel lherzolite xenolith from Oki-Dogo Island: an implication for variety of the upper mantle peridotite beneath southwest Japan. *Island Arc* **12**, 219–232.

Alibert, C. (1994). Peridotite xenoliths from western Canyon and the Thumb: a probe into the subcontinental mantle of the Colorado Plateau. *Journal of Geophysical Research* **99**, 21605–21620.

Andal, E. S., Arai, S. & Yumul, G. P., Jr (2005). The Isabela Ophiolite (Philippines): A complete mantle section of a slow spreading ridge-derived ophiolite. *Island Arc* **14**, 272–294.

Aoki, K. (1987). Japanese island arc: xenoliths in alkali basalts, high-alumina basalts, and calc-alkaline andesites and dacites. In: Nixon, P. H. (ed.) *Mantle Xenoliths*. New York: John Wiley, pp. 319–333.

Aoki, K. & Shiba, I. (1973). Pargasite in lherzolite and websterite inclusions from Itinome-gata, Japan. *Journal of Japanese Association of Mineralogy, Petrology and Economic Geology* **68**, 303–310.

Arai, S. (1980). Petrologic nature of the sub-arc lithosphere. *Earth Monthly (Gekkan Chikyu)* **2**, 822–828 (in Japanese).

Arai, S. (1984). Igneous mineral equilibria in some Alpine-type peridotites in Japan. In: Sunagawa, I. (ed.) *Materials Science in Earth's Interior*. Tokyo: Terra, pp. 445–460.

Arai, S. (1986). K/Na variation in phlogopite and amphibole of upper mantle peridotites due to fractionation of the metasomatic fluids. *Journal of Geology* **94**, 436–444.

Arai, S. (1991). Petrological characteristics of the upper mantle peridotites beneath the Japan Island Arcs—Petrogenesis of spinel peridotites. *Soviet Geology and Geophysics (Geologiya i Geofizika)* **32**, 8–26.

Arai, S. (1992). Chemistry of chromian spinel in volcanic rocks as a potential guide to magma chemistry. *Mineralogical Magazine* **56**, 173–184.

Arai, S. (1994). Characterization of spinel peridotites by olivine–spinel compositional relationships: Review and interpretation. *Chemical Geology* **113**, 191–204.

Arai, S. & Abe, N. (1994). Podiform chromitite in the arc mantle: chromitite xenoliths from the Takashima alkali basalt, southwest Japan arc. *Mineralium Deposita* **29**, 434–438.

Arai, S. & Kida, M. (2000). Origin of fine-grained peridotite xenoliths from Iraya volcano of Batan Island, Philippines: deserpentinization or metasomatism at the wedge mantle beneath an incipient arc? *Island Arc* **9**, 458–471.

Arai, S. & Takahashi, N. (1989). Formation and compositional variation of phlogopites in the Horoman peridotite complex, Hokkaido, northern Japan: implications for origin and fractionation of metasomatic fluids in the upper mantle. *Contributions to Mineralogy and Petrology* **101**, 165–175.

Arai, S., Kida, M., Abe, N., Ninomiya, A. & Yumul, G. P., Jr (1996). Classification of peridotite xenoliths in calc-alkaline andesite from Iraya volcano, Batan Island, the Philippine, and its genetical implications. *Science Reports of Kanazawa University* **41**, 25–45.

Arai, S., Abe, N. & Hirai, H. (1998). Petrological characteristics of the sub-arc mantle: An overview on petrology of peridotite xenoliths from the Japan arcs. *Trends in Mineralogy (India)* **2**, 39–55.

Arai, S., Hirai, H. & Uto, K. (2000). Mantle peridotite xenoliths from the Southwest Japan arc: a model for the sub-arc upper mantle structure and composition of the Western Pacific rim. *Journal of Mineralogical and Petrological Sciences* **95**, 9–23.

Arai, S., Abe, N., Hirai, H. & Shimizu, Y. (2001). Geological, petrological characteristics of ultramafic–mafic xenoliths in Kurose and Takashima, northern Kyushu, southwestern Japan. *Science Reports of Kanazawa University* **46**, 9–38.

Arai, S., Ishimaru, S. & Okrugin, V. M. (2003). Metasomatized harzburgite xenoliths from Avacha volcano as fragments of mantle wedge of the Kamchatka arc: an implication for the metasomatic agent. *Island Arc* **12**, 233–246.

Arai, S., Takada, S., Michibayashi, K. & Kida, M. (2004). Petrology of peridotite xenoliths from Iraya volcano, Philippines, and its implications for dynamic mantle-wedge processes. *Journal of Petrology* **45**, 369–389.

Arai, S., Kadoshima, K. & Morishita, T. (2006*a*). Widespread arc-related melting in the mantle section of the northern Oman ophiolite as inferred from detrital chromian spinels. *Journal of the Geological Society, London* **163**, 869–879.

Arai, S., Shimizu, Y., Morishita, T. & Ishida, Y. (2006*b*). A new type of orthopyroxenite xenolith from Takashima, the Southwest Japan arc: silica enrichment of the mantle by evolved alkali basalt. *Contributions to Mineralogy and Petrology* **152**, 387–398.

Arai, S., Abe, N. & Ishimaru, S. (2007). Mantle peridotites from the Western Pacific. *Gondwana Research* **11**, 180–199.

Aranda-Gómez, J. J. & Ortega-Gutiérrez, F. (1987). Mantle xenoliths in Mexico. In: Nixon, P. H. (ed.) *Mantle Xenoliths*. New York: John Wiley, pp. 75–84.

Arculus, R. J. & Wills, K. J. A. (1980). The petrology of plutonic blocks and inclusions from the Lesser Antilles Island Arc. *Journal of Petrology* **21**, 743–799.

Bali, E., Szabó, C., Vaselli, O. & Török, K. (2002). Significance of silicate melt pockets in upper mantle xenoliths from the Bakony–Balaton Highland Volcanic Field, Western Hungary. *Lithos* **61**, 79–102.

Ballhaus, C., Berry, R. F. & Green, D. H. (1990). Oxygen fugacity controls in the Earth's upper mantle. *Nature* **348**, 437–440.

Ballhaus, C., Berry, R. F. & Green, D. H. (1991). High pressure experimental calibration of the olivine–orthopyroxene–spinel oxygen geobarometer: implications for the oxidation state of the upper mantle. *Contributions to Mineralogy and Petrology* **107**, 27–40.

Barsdell, M. & Smith, I. E. M. (1989). Petrology of recrystallized ultramafic xenoliths from Morelava volcano, Vanuatu. *Contributions to Mineralogy and Petrology* **102**, 230–241.

Bjerg, E. A., Ntaflos, T., Kurat, G., Dobosi, G. & Labudía, C. H. (2005). The upper mantle beneath Patagonia, Argentina, documented by xenoliths from alkali basalts. *Journal of South American Earth Sciences* **18**, 125–145.

Blatter, D. L. & Carmichael, I. S. E. (1998). Hornblende peridotite xenoliths from central Mexico reveal the highly oxidized nature of subarc upper mantle. *Geology* **26**, 1035–1038.

Bloomer, S. H. (1983). Distribution and origin of igneous rocks from the landward slopes of the Mariana Trench; Implications for its structure and evolution. *Journal of Geophysical Research* **88**, 7411–7428.

Bloomer, S. H. & Fisher, R. L. (1987). Petrology and geochemistry of igneous rocks from the Tonga trench–A non-accreting plate boundary. *Journal of Geology* **95**, 469–495.

Bloomer, S. H. & Hawkins, J. W. (1983). Gabbroic and ultramafic rocks from the Mariana Trench: An island arc ophiolite. In: Hayes, D. E. (ed.) *The Tectonic and Geologic Evolution of Southeast Asian Seas and Islands (Part 2). Geophysical Monograph, American Geophysical Union* **27**, 294–317.

Brandon, A. L. & Draper, D. S. (1996). Constraints on the origin of the oxidation state of mantle overlying subduction zones: an example from Simcoe, Washington, USA. *Geochimica et Cosmochimica Acta* **60**, 1739–1749.

Brandon, A. L., Becker, H., Carlson, R. W. & Shirey, S. B. (1999). Isotopic constraints on time scales and mechanisms of slab material transport in the mantle wedge: evidence from the Simcoe mantle xenoliths, Washington, USA. *Chemical Geology* **160**, 387–407.

Brearley, M., Scarfe, C. M. & Fujii, T. (1984). The petrology of ultramafic xenoliths from Summit Lake, near Prince George, British Columbia. *Contributions to Mineralogy and Petrology* **88**, 53–63.

Bryant, J. A., Yogodzinski, G. M. & Churikova, T. G. (2007). Melt–mantle interaction beneath the Kamchatka arc: Evidence from ultramafic xenoliths from Shiveluch volcano. *Geochemistry, Geophysics, Geosystems* **8**, Q04007. doi: 10.1029/2006GC001443.

Canil, D. (1992). Orthopyroxene stability along the peridotite solidus and the origin of cratonic lithosphere beneath southern Africa. *Earth and Planetary Science Letters* **111**, 83–95.

Canil, D. & Scarfe, C. M. (1989). Origin of phlogopite in mantle xenoliths from Kostal Lake, Wells Gray Park, British Columbia. *Journal of Petrology* **30**, 1159–1179.

Cardwell, R. K., Isacks, B. L. & Karig, D. E. (1980). The spatial distribution of earthquakes, focal mechanism solutions, and subducted lithosphere in the Philippine and northeastern Indonesian islands. In: Hayes, D. E. (ed.) *The Tectonic and Geologic Evolution of Southeast Asian Seas and Islands. Geophysical Monograph, American Geophysical Union* **23**, 1–35.

Conceição, R. V., Mallmann, G., Koeser, E., Schilling, M., Bertotto, G. W. & Rodriguez-Vergas, A. (2005). Andean subduction-related mantle xenoliths: Isotopic evidence of Sr–Nd decoupling during metasomatism. *Lithos* **82**, 273–287.

Conrad, W. K. & Kay, R. W. (1984). Ultramafic and mafic inclusions from Adak Island: Crystallization history, and implications for the nature of primary magmas and crust evolution in the Aleutian arc. *Journal of Petrology* **25**, 88–125.

Cooper, P. & Taylor, B. (1989). Seismicity and focal mechanisms at the New Britain Trench related to deformation of the lithosphere. *Tectonophysics* **164**, 25–40.

Csontos, L. (1995). Tertiary tectonic evolution of the Intra-Carpathian area: a review. *Acta Volcanologica* **7**, 1–13.

Csontos, L. & Vörös, A. (2004). Mesozoic plate tectonic reconstruction of the Carpathian region. *Palaeogeography, Palaeoclimatology, Palaeoecology* **210**, 1–56.

Debari, S., Kay, S. M. & Kay, R. W. (1987). Ultramafic xenoliths from Adagdak volcano, Adak, Aleutian Islands, Alaska: Deformed igneous cumulates from the Moho of an island arc. *Journal of Geology* **95**, 329–341.

DeLong, S. E., Hodges, F. N. & Arculus, R. J. (1975). Ultramafic and mafic inclusions, Kanaga Island, Alaska, and the occurrence of alkaline rocks in island arcs. *Journal of Geology* **83**, 721–736.

Demény, A., Vennemann, T. W., Hegner, E., Nagy, G., Milton, J. A., Embey-Isztin, A., Homonnay, Z. & Dobosi, G. (2004). Trace-element and C–O–Sr–Nd isotope evidence for subduction-related carbonate–silicate melts in mantle xenoliths (Pannonian Basin, Hungary). *Lithos* **75**, 89–113.

DeMets, C., Gordon, R., Argus, D. & Stein, S. (1990). Current plate motions. *Geophysical Journal International* **101**, 425–478.

Dewey, J. F. & Lamb, S. H. (1992). Active tectonics of the Andes. *Tectonophysics* **205**, 79–95.

Dick, H. J. B. & Bullen, T. (1984). Chromian spinel as a petrogenetic indicator in abyssal and alpine type peridotites and spatially associated lavas. *Contributions to Mineralogy and Petrology* **86**, 54–76.

Dick, H. J. B., Fisher, R. L. & Bryan, W. B. (1984). Mineralogic variability of the uppermost mantle along mid-ocean ridge. *Earth and Planetary Science Letters* **69**, 88–106.

Dobosi, G., Kurat, G., Jenner, G. A. & Brandstätter, F. (1999). Cryptic metasomatism in the upper mantle beneath Southeastern Austria: a laser ablation microprobe-ICP-MS study. *Mineralogy and Petrology* **67**, 143–161.

Downes, H., Vaselli, O., Seghedi, I., Ingram, G., Rex, D., Coradossi, N., Pécskay, Z. & Pinarelli, L. (1995). Geochemistry of late Cretaceous–early Tertiary magmatism in Poiana Rusca (Romania). *Acta Volcanologica* **7**, 209–217.

Downes, H., Macdonald, R., Upton, B. G. J., Cox, K. G., Bodinier, J.-L., Mason, P. R. D., James, D., Hill, P. G. & Hearn, B. C., Jr (2004). Ultramafic xenoliths from the Bearpaw Mountains, Montana, USA: evidence for multiple metasomatic events in the lithospheric mantle beneath the Wyoming craton. *Journal of Petrology* **45**, 1631–1662.

Draper, D. S. (1992). Spinel lherzolites from Lorena Butte, Simcoe Mountains, southern Washington (USA). *Journal of Geology* **100**, 766–776.

Ducea, M. & Saleeby, J. (1998). Crustal recycling beneath continental arc: silica-rich glass inclusions in ultramafic xenoliths from the Sierra Nevada, California. *Earth and Planetary Science Letters* **156**, 101–116.

Ehrenberg, S. N. (1979). Garnetiferous ultramafic inclusions in minette from the Navajo Volcanic Field. In: Boyd, F. R. & Meyer, H. O. A (eds) *The Mantle Sample: Inclusions in Kimberlites and Other Volcanics. Geophysical Monograph, American Geophysical Union* 330–344.

Ehrenberg, S. N. (1982). Petrogenesis of garnet lherzolite and megacrystalline nodules from The Thumb, Novajo Volcanic Field. *Journal of Petrology* **23**, 507–547.

Embey-Isztin, A., Dobosi, G., Altherr, R. & Meyer, H.-P. (2001). Thermal evolution of the lithosphere beneath the western Pannonian Basin: evidence from deep-seated xenoliths. *Tectonophysics* **331**, 285–306.

Ertan, I. E. & Leeman, W. P. (1996). Metasomatism of Cascades subarc mantle: evidence from a rare phlogopite orthopyroxenite xenolith. *Geology* **24**, 451–454.

Faure, M. & Natal'n, B. (1992). The geodynamic evolution of the eastern Eurasian margin in Mesozoic times. *Tectonophysics* **208**, 397–411.

Fisher, R. L. & Engel, C. G. (1969). Ultramafic and basaltic rocks dredged from the nearshore flank of the Tonga trench. *Geological Society of America Bulletin* **80**, 1373–1378.

Fitch, T. J. (1972). Plate convergence, transcurrent faults, and internal deformation adjacent to Southeast Asia and the Western Pacific. *Journal of Geophysical Research* **77**, 4432–4460.

Forbes, W. C. & Flower, M. F. J. (1974). Phase relations of titan-phlogopite, $K_2Mg_4TiAl_2Si_6O_{22}(OH)_4$: a refractory phase in the upper mantle. *Earth and Planetary Science Letters* **22**, 60–66.

Francis, D. M. (1976*a*). The origin of amphibole in lherzolite xenoliths from Nunivak Island, Alaska. *Journal of Petrology* **17**, 357–378.

Francis, D. M. (1976*b*). Amphibole pyroxenite xenoliths: cumulate or replacement phenomena from the upper mantle, Nunivak Island, Alaska. *Contributions to Mineralogy and Petrology* **58**, 51–61.

Francis, D. (1987). Mantle–melt interaction recorded in spinel lherzolite xenoliths from the Alligator Lake Volcanic Complex, Yukon, Canada. *Journal of Petrology* **28**, 569–597.

Franz, L. & Wirth, R. (2000). Spinel inclusions in olivine of peridotite xenoliths from TUBAF seamount (Bismarck Archipelago/Papua New Guinea): evidence for the thermal and tectonic evolution of the oceanic lithosphere. *Contributions to Mineralogy and Petrology* **140**, 283–295.

Franz, L., Becker, K.-P., Kramer, W. & Herzig, P. M. (2002). Metasomatic mantle xenoliths from the Bismarck microplate (Papua New Guinea)—Thermal evolution, geochemistry and extent of slab-induced metasomatism. *Journal of Petrology* **43**, 315–343.

Frey, F. A. & Prinz, M. (1978). Ultramafic inclusions from San Carlos, Arizona: petrologic and geochemical data bearing on their petrogenesis. *Earth and Planetary Science Letters* **38**, 129–176.

Fryer, P. (1996). Evolution of the Mariana convergent plate margin system. *Review of Geophysics* **34**, 89–125.

Fujii, T. & Scarfe, C. M. (1982). Petrology of ultramafic nodules from West Kettle river, near Kelowna, southern British Columbia. *Contributions to Mineralogy and Petrology* **80**, 297–306.

Gilbert, M. C. (1969). Reconnaissance study of the stability of amphiboles at high pressures. *Carnegie Institution of Washington Yearbook* **67**, 167–170.

Gilbert, M. C., Hlet, R. T., Popp, R. K. & Spear, F. S. (1982). Experimental studies of amphibole stability. In: Veblen, D. R. & Ribbe, P. H. (eds) *Amphiboles: Petrology and Experimental Phase Relations. Mineralogical Society of America, Reviews in Mineralogy* **9B**, 229–353.

Gorbatov, A., Kostoglodov, V., Suárez, G. & Gordeev, E. (1997). Seismicity and structure of the Kamchatka subduction zone. *Journal of Geophysical Research* **102**, 17883–17898.

Gorring, M. L. & Kay, S. M. (2000). Carbonatite metasomatized peridotite xenoliths from southern Patagonia: implications for lithospheric processes and Neogene plateau magmatism. *Contributions to Mineralogy and Petrology* **140**, 55–72.

Gorring, M. L. & Kay, S. M. (2001). Mantle processes and sources of Neogene slab window magmas from Southern Patagonia, Argentina. *Journal of Petrology* **42**, 1067–1094.

Goto, K. & Arai, S. (1987). Petrology of peridotite xenoliths in lamprophyre from Shingu, Southwestern Japan: implications for origin of Fe-rich mantle peridotite. *Mineralogy and Petrology* **37**, 137–155.

Harder, M. & Russell, J. K. (2006). Thermal state of the upper mantle beneath the Northern Cordilleran Volcanic Province (NCVP), British Columbia, Canada. *Lithos, Mantle to Magma—Lithospheric and Volcanic Processes in Western North America* **87**, 1–22.

Harte, B. (1977). Rock nomenclature with pariticular relations to deformation and recrystallization textures in olivine-bearing xenoliths. *Journal of Geology* **85**, 279–288.

Hattori, K., Arai, S. & Clarke, B. (2002). Selenium, tellurium, arsenic and antimony contents in primary mantle sulphides. *Canadian Mineralogist* **40**, 637–650.

Heinrich, W. & Besch, T. (1992). Thermal history of the upper mantle beneath a young back-arc extensional zone: ultramafic xenoliths from San Luis Potosí, Central Mexico. *Contributions to Mineralogy and Petrology* **111**, 126–142.

Hirai, H. (1986). Petrology of ultramafic xenoliths from Noyamadake and Kurose, southwestern Japan. PhD thesis, University of Tsukuba.

Holloway, J. R. (1973). The system pargasite–H_2O–CO_2: a model for melting of a hydrous mineral with a mixed-volatile fluid—I. Experimental results to 8 kbar. *Geochimica et Cosmochimica Acta* **37**, 651–666.

Ikehata, K. & Arai, S. (2004). Metasomatic formation of kosmochlor-bearing diopside in peridotite xenoliths from North Island, New Zealand. *American Mineralogist* **89**, 1396–1404.

Ionov, D. A., Prikhod'ko, V. S. & O'Reilly, S. Y. (1995). Peridotite xenoliths in alkali basalts from the Sikhote-Alin, southeastern Siberia, Russia: trace-element signatures of mantle beneath a convergent continental margin. *Chemical Geology* **120**, 275–294.

Ishii, T. (1985). Dredged samples from the Ogasawara fore-arc seamount or 'Ogasawara Paleoland'—'fore-arc ophiolite'. In: Nasu, N., Kobayashi, K., Uyeda, S., Kushiro, I. & Kagami, H. (eds) *Formation of Active Ocean Margin*. Tokyo: TERRAPUB, pp. 307–342.

Ishii, T., Robinson, P. T., Maekawa, H. & Fiske, R. (1992). Petrological studies of peridotites from diapiric serpentinite seamounts in the Izu–Ogasawara–Mariana forearc, Leg 125. In: Fryer, P., Pearce, J. A. & Stokking, L. B. *et al.* (eds) *Proceedings of the Ocean Drilling Program, Scientific Results, 125*. College Station, TX: Ocean Drilling Program, pp. 445–485.

Ishii, T., Sato, H., Haraguchi, S, Frayer, P., Fujioka, K., Bloomer, S. & Yokose, H. (2000). Petrological characteristics of peridotites from serpentinite seamounts in the Izu–Ogasawara–Mariana forearc. *Journal of Geography (Tokyo)* **109**, 517–530 (in Japanese with English abstract).

Ishimaru, S. (2004). The petrological characters of mantle wedge beneath Kamchatka arc. Master's thesis, Kanazawa University.

Ishimaru, S. & Arai, S. (2008). Calcic amphiboles in peridotite xenoliths from Avacha volcano, Kamchatka, and their implications for metasomatic conditions in the mantle wedge. In: Coltorti, M. & Grégoire, M. (eds) *Metasomatism in Oceanic and Continental Lithospheric Mantle. Geological Society, London, Special Publications* **293**, 35–55.

Ishimaru, S., Arai, S., Ishida, Y., Shirasaka, M. & Okrugin, V. M. (2007). Melting and multi-stage metasomatism in the mantle wedge beneath a frontal arc inferred from highly depleted peridotite xenoliths from the Avacha volcano, southern Kamchatka. *Journal of Petrology* **48**, 395–433.

Iwamori, H. (1991). Zonal structure of Cenozoic basalts related to mantle upwelling in southwest Japan. *Journal of Geophysical Research* **96**, 6157–6170.

Karig, D. E. (1971). Origin and development of marginal basins in the western Pacific. *Journal of Geophysical Research* **76**, 2542–2561.

Kay, S. M. & Kay, R. W. (1986). Role of crystal cumulates and the oceanic crust in the formation of the lower crust of the Aleutian arc. *Geology* **13**, 461–464.

Kelemen, P. B. (1990). Reaction between ultramafic wall rock and fractionating basaltic magma, I. Phase relations, the origin of calc-alkaline magma series, and the formation of discordant dunite. *Journal of Petrology* **31**, 51–98.

Kelemen, P. B., Hart, S. R. & Bernstein, S. (1998). Silica enrichment in the continental upper mantle via melt/rock reaction. *Earth and Planetary Science Letters* **164**, 387–406.

Kepezhinskas, P. K. & Defant, M. J. (2001). Nonchondritic Pt/Pd ratios in arc mantle xenoliths: Evidence for platinum enrichment in depleted island-arc mantle sources. *Geology* **29**, 851–854.

Kepezhinskas, P. K., Defant, M. J. & Drummond, M. S. (1995). Na metasomatism in the sub-arc mantle by slab melt–peridotite interaction: evidence from mantle xenoliths in the Kamchatka arc. *Journal of Petrology* **36**, 1505–1527.

Keppler, H. (1996). Constraints from partitioning experiments on the composition of subduction-zone fluids. *Nature* **380**, 237–240.

Kesson, S. E. & Ringwood, A. E. (1989). Slab–mantle interactions 2. The formation of diamonds. *Chemical Geology* **78**, 97–118.

Kida, M. (1998). Peridotite xenoliths from Iraya volcano, the Philippines: Metasomatized peridotite beneath the immature arc. Master's thesis, Kanazawa University.

Kilian, R. & Stern, C. R. (2002). Constraints on the interaction between slab melts and the mantle wedge from adakitic glass in peridotite xenoliths. *European Journal of Mineralogy* **14**, 25–36.

Kimura, J. & Yoshida, T. (2006). Contributions of slab fluid, mantle wedge and crust to the origin of Quaternary lavas in the NE Japan arc. *Journal of Petrology* **47**, 2185–2232.

Konečný, P., Konečný, V., Lexa, J. & Huraiová, M. (1995). Mantle xenoliths in alkali basalts of Southern Slovakia. *Acta Volcanologica* **7**, 241–247.

Konzett, J. & Ulmer, P. (1999). The stability of hydrous potassic phases in lherzolitic mantle—an experimental study to 9·5 GPa in simplified and natural bulk compositions. *Journal of Petrology* **40**, 629–652.

Kuno, H. (1966). Lateral variation of basalt magma across continental margins and island arcs. *Bulletin Volcanologique* **29**, 195–222.

Kushiro, I., Syono, Y. & Akimoto, S. (1967). Stability of phlogopite at high pressures and possibly presence of phlogopite in the Earth's upper mantle. *Earth and Planetary Science Letters* **3**, 197–203.

Laurora, A., Mazzucchelli, M., Rivalenti, G., Vannucci, R., Zanetti, A., Barbieri, M. A. & Cingolani, C. A. (2001). Metasomatism and melting in carbonated peridotite xenoliths from the mantle wedge: the Gobernador Gregores case (Southern Patagonia). *Journal of Petrology* **42**, 69–87.

Lee, D.-W. (1999). Strike-slip fault tectonics and basin formation during the Cretaceous in the Korean Peninsula. *Island Arc* **8**, 218–231.

Lewis, S. D. & Hayes, D. E. (1989). Plate convergence and deformation, North Luzon Ridge, Philippines. *Tectonophysics* **168**, 221–237.

Littlejohn, A. L. & Greenwood, H. J. (1974). Lherzolite nodules in basalts from British Columbia, Canada. *Canadian Journal of Earth Sciences* **11**, 1288–1308.

Lucassen, F., Franz, G., Viramonte, J., Romer, R. L., Dulski, P. & Lang, A. (2005). The late Cretaceous lithospheric mantle beneath the Central Andes: Evidence from phase equilibria and composition of mantle xenoliths. *Lithos* **82**, 379–406.

Luhr, J. F. & Aranda-Gómez, J. J. (1997). Mexican peridotite xenoliths and tectonic terranes: correlations among vent location, texture, temperature, pressure, and oxygen fugacity. *Journal of Petrology* **38**, 1075–1112.

Maury, R. C., Defant, M. & Joron, J.-L. (1992). Metasomatism of the sub-arc mantle inferred from trace elements in Philippine xenoliths. *Nature* **360**, 661–663.

McInnes, B. I. A. & Cameron, E. M. (1994). Carbonated, alkaline hybridizing melts from a sub-arc environment: Mantle wedge

samples from the Tabar–Lihir–Tanga–Feni arc, Papua New Guinea. *Earth and Planetary Science Letters* **122**, 125–141.

McInnes, B. I. A., Grégoire, M., Binns, R. A., Herzig, P. M. & Hannington, M. D. (2001). Hydrous metasomatism of oceanic sub-arc mantle, Lihir, Papua New Guinea: petrology and geochemistry of fluid-metasomatised mantle wedge xenoliths. *Earth and Planetary Science Letters* **188**, 169–183.

Menzies, M. A., Arculus, R. J., Best, M. G., Bergman, S. C., Ehrenberg, S. N., Irving, A. J., Roden, M. F. & Schulze, D. J. (1987). A record of subduction process and within-plate volcanism in lithospheric xenoliths of the southwestern USA. In: Nixon, P. H. (ed.) *Mantle Xenoliths*. New York: John Wiley, pp. 59–74.

Mercier, J. C. & Nicolas, A. (1975). Textures and fabrics of upper-mantle peridotites as illustrated by xenoliths from basalts. *Journal of Petrology* **16**, 454–487.

Meyer, H. O. A. & Svisero, D. P. (1987). Mantle xenoliths in South America. In: Nixon, P. H. (ed.) *Mantle Xenoliths*. New York: John Wiley, pp. 85–91.

Mibe, K., Fujii, T. & Yasuda, A. (2002). Composition of aqueous fluid coexisting with mantle minerals at high pressure and its bearing on the differentiation of the Earth's mantle. *Geochimica et Cosmochimica Acta* **66**, 2273–2285.

Minster, J. B., Jordan, T. H., Molnar, P. & Haines, E. (1974). Numerical modelling of instantaneous plate tectonics. *Geophysical Journal of the Royal Astronomical Society* **36**, 541–576.

Mitchell, R. H. (1987). Mantle-derived xenoliths in Canada. In: Nixon, P. H. (ed.) *Mantle Xenoliths*. New York: John Wiley, pp. 33–40.

Nakamura, E., McCulloch, M. T. & Campbell, I. H. (1990). Chemical geodynamics in the back-arc region of Japan based on the trace element and Sr–Nd isotopic compositions. *Tectonophysics* **174**, 207–233.

Nakamura, Y. & Kushiro, I. (1974). Composition of the gas phase in Mg_2SiO_4–SiO_2–H_2O at 15 kbar. *Carnegie Institution of Washington Yearbook* **73**, 255–258.

Niida, K. & Green, D. H. (1999). Stability and chemical composition of pargasitic amphibole in MORB pyrolite under upper mantle conditions. *Contributions to Mineralogy and Petrology* **135**, 18–40.

Ninomiya, A. & Arai, S. (1992). Harzburgite fragment in a composite xenolith from an Oshima-Ôshima andesite, the Northeast Japan arc. *Bulletin of the Volcanological Society of Japan* **37**, 269–273 (in Japanese).

Ninomiya, C., Arai, S. & Ishii, T. (2007). Peridotite xenoliths from the Takeshima seamount, Japan: an insight into the upper mantle beneath the Sea of Japan. *Japanese Magazine of Mineralogical and Petrological Sciences* **36**, 1–14 (in Japanese with English abstract).

Nixon, P. H. (ed.) (1987). *Mantle Xenoliths*. New York: John Wiley, 844 p.

Ohara, Y. & Ishii, T. (1998). Peridotites from the southern Mariana forearc: Heterogeneous fluid supply in the mantle wedge. *Island Arc* **7**, 541–558.

Okamura, H., Arai, S. & Kim, Y.-U. (2006). Petrology of fore-arc peridotite from the Hahajima Seamount, the Izu–Bonin arc, with special reference to chemical characteristics of chromian spinel. *Mineralogical Magazine* **70**, 15–26.

Otofuji, Y., Mastuda, T. & Nohda, S. (1985). Paleomagnetic evidence for the Miocene counter-clockwise rotation of Northeast Japan—rifting process of the Japan Sea. *Earth and Planetary Science Letters* **75**, 265–277.

Parkinson, I. J. & Arculus, R. J. (1999). The redox state of subduction zone: insights from arc peridotites. *Chemical Geology* **160**, 409–423.

Parkinson, I. J. & Pearce, J. A. (1998). Peridotites from the Izu–Bonin–Mariana forearc (ODP Leg 125): Evidence for mantle melting and melt–mantle interaction in a supra-subduction zone setting. *Journal of Petrology* **39**, 1577–1618.

Parkinson, I. J., Arculus, R. J. & Eggins, S. M. (2003). Peridotite xenoliths from Grenada, Lesser Antilles Island Arc. *Contributions to Mineralogy and Petrology* **146**, 241–262.

Pearce, J. A. & Cann, J. R. (1973). Tectonic setting of basic volcanic rocks investigated using trace element analyses. *Earth and Planetary Science Letters* **19**, 290–300.

Pearce, J. A., Barker, P. F., Edwards, S. J., Parkinson, I. J. & Leat, P. T. (2000). Geochemistry and tectonic significance of peridotites from the South Sandwich arc–basin system, South Atlantic. *Contributions to Mineralogy and Petrology* **139**, 36–53.

Peslier, A. H., Francis, D. & Ludden, J. (2002). The lithospheric mantle beneath continental margins: melting and melt–rock reaction in Canadian Cordillera xenoliths. *Journal of Petrology* **43**, 2013–2047.

Quick, J. E. (1981). The origin and significance of large, tabular dunite bodies in the Trinity Peridotite, northern California. *Contributions to Mineralogy and Petrology* **78**, 413–422.

Ramos, V. A. (1999). Plate tectonic setting of the Andean Cordillera. *Episodes* **22**, 183–190.

Ramos, V. A. & Kay, S. M. (1992). Southern Patagonian plateau basalts and deformation: backarc testimony of ridge collisions. *Tectonophysics* **205**, 261–282.

Ramos, V. A., Niemeyer, H., Skarmeta, J. & Munoz, J. (1982). Magmatic evolution of the Austral Patagonian Andes. *Earth-Science Reviews* **18**, 411–443.

Richard, M. (1986). Géologie et pétrologie d'un jalon de l'Arc Taïwan–Luzon: L'Ile de Batan (Philippines). PhD thesis, University of Bretagne Occidentale, Brest, France.

Riter, J. C. A. & Smith, D. (1996). Xenolith constraints on the thermal history of the mantle below the Colorado Plateau. *Geology* **24**, 267–270.

Rivalenti, G., Mazzucchelli, M., Laurora, A., Ciuffi, S. I. A., Zanetti, A., Vannucci, R. & Cingolani, C. A. (2004*a*). The backarc mantle lithosphere in Patagonia, South America. *Journal of South American Earth Sciences* **17**, 121–152.

Rivalenti, G., Zanetti, A., Mazzucchelli, Vannucci, R. & Cingolani, C. A. (2004*b*). Equivocal carbonatite markers in the mantle xenoliths of the Patagonia backarc: the Gobernador Gregores case (Santa Cruz Province, Argentina). *Contributions to Mineralogy and Petrology* **147**, 647–670.

Rodriguez-Vargas, A., Koester, E., Mallmann, G., Conceição, R. V., Kawashita, K. & Weber, M. B. I. (2005). Mantle diversity beneath the Colombian Andes, Northern Volcanic Zone: Constraints from Sr and Nd isotopes. *Lithos* **82**, 471–484.

Schilling, M., Conceição, R. V., Mallmann, G., Koester, E., Kawashita, K., Hervé, F., Morata, D. & Motoki, A. (2005). Spinel-facies mantle xenoliths from Cerro Redondo, Argentine Patagonia: petrographic, geochemical, and isotopic evidence of interaction between xenoliths and host basalt. *Lithos* **82**, 485–502.

Shi, L., Francis, D., Ludden, J., Frederiksen, A. & Bostock, M. (1998). Xenolith evidence for lithospheric melting above anomalously hot mantle under the northern Canadian Cordillera. *Contributions to Mineralogy and Petrology* **131**, 39–53.

Smith, D. (1979). Hydrous minerals and carbonates in peridotite inclusions from the Green Knobs and Buell Park kimberlitic diatremes on the Colorado Plateau. In: Boyd, F. R. & Meyer, H. O. A. (eds) *The Mantle Sample: Inclusions in Kimberlites*

and Other Volcanics. Geophysical Monograph, American Geophysical Union 345–356.

Smith, D. (2000). Insights into the evolution of the uppermost continental mantle from xenolith localities on and near the Colorado Plateau and regional comparisons. *Journal of Geophysical Research* **105**, 16769–16781.

Smith, D. & Riter, J. C. A. (1997). Genesis and evolution of low-Al orthopyroxene in spinel peridotite xenoliths, Grand Canyon field, Arizona, USA. *Contributions to Mineralogy and Petrology* **127**, 391–404.

Smith, D., Riter, J. C. A. & Merzman, S. A. (1999). Erratum to 'Water–rock interactions, orthopyroxene growth, and Si-enrichment in the mantle: evidence in xenoliths from the Colorado Plateau, southwestern United States'. *Earth and Planetary Science Letters* **167**, 347–356.

Stern, C. R., Frey, F. A., Futa, K., Zartman, R. F., Peng, Z. & Kyser, T. K. (1990). Trace-element and Sr, Nd, Pf, and O isotopic composition of Pliocene and Quaternary alkali basalts of the Patagonian Plateau lavas of southernmost South America. *Contributions to Mineralogy and Petrology* **104**, 294–308.

Stern, C. R., Kilian, R., Oiker, B., Hauri, E. H. & Kyser, T. K. (1999). Evidence from mantle xenoliths for relatively thin (<100 km) continental lithosphere below the Phanerozoic crust of southernmost South America. *Lithos* **48**, 217–235.

Sugimura, A., Matsuda, T., Chinzei, K. & Nakamura, K. (1963). Quantitative distribution of late Cenozoic volcanic materials in Japan. *Bulletin Volcanologique* **26**, 125–140.

Swanson, S. E., Kay, S. M., Brearley, M. & Scarfe, C. M. (1987). Arc and back-arc xenoliths in Kurile–Kamchatka and western Alaska. In: Nixon, P. H. (ed.) *Mantle Xenoliths*. New York: John Wiley, pp. 303–318.

Szabó, Cz. & Taylor, L. A. (1994). Mantle petrology and geochemistry beneath the Nógrád–Gömör Volcanic Field, Carparthian–Pannonian Region. *International Geology Review* **36**, 328–358.

Szabó, Cs., Harangi, S. & Csontos, L. (1992). Review of Neogene and Quaternary volcanism of the Carpathian–Pannonian region. *Tectonophysics* **208**, 243–256.

Szabó, C., Vaselli, O., Vannucci, R., Bottazzi, P., Ottolini, L., Coradossi, N. & Kubovics, I. (1995). Ultramafic xenoliths from the Little Hungarian Plain (Western Hungary): a petrologic and geochemical study. *Acta Vulcanologica* **7**, 249–263.

Szabó, Cs., Bodnar, R. J. & Sobolev, A. V. (1996). Metasomatism associated with subduction-related, volatile-rich silicate melt in the upper mantle beneath the Nógrád–Gómór Volcanic Field, Northern Hungary/Southern Slovakia: Evidence from silicate melt inclusions. *European Journal of Mineralogy* **8**, 881–899.

Szabó, Cz., Fauls, G., Zajacz, Z., Kovacs, I. & Bali, E. (2004). Composition and evolution of lithosphere beneath the Carpathian–Pannonian region: a review. *Tectonophysics* **393**, 119–137.

Takahashi, E. (1978*a*). Petrological model of the crust and upper mantle of the Japanese island arcs. *Bulletin Volcanologique* **41**, 529–547.

Takahashi, E. (1978*b*). Petrology of ultramafic and mafic xenoliths in Cenozoic alkali basalts of Oki-Dogo Island in the Japan Sea. PhD thesis, University of Tokyo.

Takahashi, E. (1980). Thermal history of lherzolite xenoliths—I. Petrology of lherzolite xenoliths from the Ichinomegata crater, Oga Peninsula, northeast Japan. *Geochimica et Cosmochimica Acta* **44**, 1643–1658.

Takahashi, E. (1986). Genesis of calc-alkali andesite magma in a hydrous mantle–crust boundary: petrology of lherzolite xenoliths from the Ichinomegata crater, Oga Peninsula, Northeast Japan, part II. *Journal of Volcanology and Geothermal Research* **29**, 355–395.

Takamura, H. (1973). Petrographical and petrochemical studies of the Cenozoic basaltic rocks on Chugoku Province. *Geological Report of Hiroshima University* **18**, 1–167 (in Japanese with English abstract).

Tamaki, K. & Honza, E. (1991). Global tectonics and formation of marginal basins: Role of the western Pacific. *Episodes* **14**, 224–230.

Tatsumi, Y. (1986). Formation of the volcanic front in subduction zones. *Geophysical Research Letters* **13**, 717–720.

Tatsumi, Y., Sakuyama, M., Fukuyama, H. & Kushiro, I. (1983). Generation of arc basalt magmas and thermal structure of the mantle wedge in subduction zones. *Journal of Geophysical Research* **88**, 5815–5825.

Tatsumi, Y., Furukawa, Y., Kogiso, T., Yamanaka, Y., Yokoyama, T. & Fedotov, S. A. (1994). A third volcanic chain in Kamchatka: thermal anomaly at transform/convegence plate boundary. *Geophysical Research Letters* **21**, 537–540.

Turner, S. P., Peate, D. W., Hawkesworth, C. J., Eggins, S. M. & Crawford, A. J. (1999). Two mantle domains and the time scales of fluid transfer beneath the Vanuatu arc. *Geology* **27**, 963–966.

Uto, K. (1990). Neogene volcanism of Southwest Japan: its time and space on K–Ar dating. PhD thesis, University of Tokyo.

Uyeda, S. & Kanamori, H. (1979). Back-arc opening and the mode of subduction. *Journal of Geophysical Research* **84**, 1049–1061.

van Ufford, A. Q. & Cloos, M. (2005). Cenozoic tectonics of New Guinea. *AAPG Bulletin* **89**, 119–140.

Vaselli, O., Downes, H., Thirlwall, M., Dobosi, G., Coradossi, N., Seghedi, I., Szakacs, A. & Vannucci, R. (1995). Ultramafic xenoliths in Plio-Pleistocene alkali basalts from the Eastern Transylvanian basin: depleted mantle enriched by vein metasomatism. *Journal of Petrology* **36**, 23–53.

Vidal, P., Dupuy, C., Maury, R. & Richard, M. (1989). Mantle metasomatism above subduction zones: trace-element and radiogenic isotope characteristics of peridotite xenoliths from Batan island (Philippines). *Geology* **17**, 1115–1118.

Wallace, L. M., Stevens, C., Silver, E., McCaffrey, R., Loratung, W., Hasiata, S., Stanaway, R., Curley, R., Rosa, R. & Taugaloidi, J. (2004). GPS and seismological constraints on active tectonics and arc–continent collision in Papua New Guinea: Implications for mechanics of microplate rotations in a plate boundary zone. *Journal of Geophysical Research* **109**, doi:10.1029/2003JB002481.

Wells, P. R. A. (1977). Pyroxene thermometry in simple and complex systems. *Contributions to Mineralogy and Petrology* **62**, 129–139.

Xu, J., Tong, W., Zhu, G., Lin, S. & Ma, G. (1989). An outline of the pre-Jurassic tectonic framework in east Asia. *Journal of Southeast Asian Earth Sciences* **3**, 29–45.

Yamamoto, J., Kaneoka, I., Nakai, S., Kagi, H., Prikhod'ko, V. S. & Arai, S. (2004). Extremely low $^{3}He/^{4}He$ and relatively low $^{40}Ar/^{36}Ar$ ratios observed in ultramafic mantle xenoliths from Far Eastern Russia: Evidence for incorporation of recycled components into the subcontinental mantle. *Chemical Geology* **207**, 237–259.

Yaxley, G. M. & Green, D. H. (1996). Experimental reconstruction of sodic dolomitic carbonatite melts from metasomatised lithosphere. *Contributions to Mineralogy and Petrology* **124**, 359–369.

Yaxley, G. M., Crawford, A. J. & Green, D. H. (1991). Evidence for carbonatite metasomatism in spinel peridotite xenoliths from western Victoria, Australia. *Earth and Planetary Science Letters* **107**, 305–317.

Yoshii, T. (1979). A detailed cross-section of the deep sesmic zone beneath northeastern Honshu, Japan. *Tectonophysics* **55**, 349–360.

Zanetti, A., Vannucci, R., Oberti, R. & Dobosi, G. (1995). Trace-element composition and crystal-chemistry of mantle amphiboles from the Carpatho-Pannonian region. *Acta Volcanologica* **7**, 265–276.